Review Article

Hydrogel-driven construction of integrated cancer theranostic platforms: From diagnosis to therapy

Xuanming Mao[1,2#], Mingyu Cui[1,2#], Lu-Qi Cao[2], Yating Zhao[3], Yuhao Xie[2], Liying Cai[3], Xiang Chen[2], Ye Liu[1], Shanzhi Wang[2]*, Zhe-Sheng Chen[2]*, Guogui Sun[1,4]*

[1]North China University of Science and Technology Affiliated Hospital, Tangshan 063210, Hebei, China.

[2]Department of Pharmaceutical Sciences, College of Pharmacy and Health Sciences, St. John's University, Queens 11439, NY, USA.

[3]Department of Breast Center, North China University of Science and Technology Affiliated Hospital, Tangshan 063210, Hebei, China.

[4]Hebei Provincial Key Laboratory of Medical-Engineering Integration Precision Medicine, Tangshan 063000, Hebei, China.

[#]These authors contributed equally to the work, and serve as co-first authors.

Correspondence to: Dr. Shanzhi Wang, Dr. Zhe-Sheng Chen, Department of Pharmaceuti cal Sciences, College of Pharmacy and Health Sciences, St. John's University, Queens 114 39, NY, USA. Email: wangs1@stjohns.edu, chenz@stjohns.edu; Dr. Guogui Sun, North Ch ina University of Science and Technology Affiliated Hospital, Tangshan 063210, Hebei, Ch ina. Email: guogui_sun2021@sina.com

Received: 09 June 2026 | Approved: 23 June 2026 | Online: 23 June 2026

Abstract

© The Author(s) 2026. Open Access This article is licensed under a Creative Commons Attribution 4.0 International License (https://creativecommons.org/licenses/by/4.0/), which permits unrestricted use, sharing, adaptation, distribution and reproduction in any medium or format, for any purpose, even commercially, as long as you give appropriate credit to the original author(s) and the source, provide a link to the Creative Commons license, and indicate if changes were made.

Current cancer treatment still relies largely on stage-specific diagnosis and relatively fixed therapeutic regimens, with diagnostic information, therapeutic intervention, and efficacy feedback often separated into different time windows, making it increasingly difficult to meet the demands of precision and individualized therapy. Theranostic platforms can organically integrate disease diagnosis with therapeutic decision-making. They can simultaneously provide feedback on or predict therapeutic efficacy during treatment, thereby enabling continuous evaluation throughout the entire treatment course. Hydrogels, as a class of soft materials with tissue-like three-dimensional networks, can stably load imaging probes and therapeutic agents by virtue of their unique biological characteristics, while also enabling controlled release, signal activation, and therapeutic monitoring at lesion sites, thus providing an ideal material basis for the construction of integrated cancer theranostic platforms. This review systematically summarizes hydrogel construction strategies for different diagnostic and therapeutic scenarios, with particular emphasis on the practical impact of distinct matrix compositions, crosslinking modes, and emerging materials on hydrogel-based theranostic platforms. We further highlight recent advances over the past three years in precision oncology and, on this basis, discuss in depth the key applications of hydrogels in tumor biomarker recognition and enrichment, visual imaging, therapeutic payload delivery, and multifunctional integration. Finally, we analyze the challenges facing practical implementation in this field and outline future directions involving organoids, spatial omics, artificial intelligence, and bioelectronic interfaces, with the aim of providing a systematic reference for the design of next-generation hydrogel-based cancer theranostic platforms that are personalized, monitorable, and clinically translatable.

Keywords: Hydrogels, cancer, diagnosis, therapy, theranostic platforms

INTRODUCTION

Cancer has become one of the leading causes of death and disease burden worldwide. According to estimates from the World Health Organization/International Agency for Research on Cancer (WHO/IARC), there were approximately 21.3 million new cancer cases and 10.4 million cancer-related deaths globally in 2025 alone[1]. As the global cancer

burden intensifies,conventional clinical pathways that distribute diagnosis, treatment, and efficacy feedback across separate time windows are increasingly unable to meet the demands for precision and timeliness in oncologic care. Precision oncology emphasizes delivering the right treatment to the right patient at the right time[2]. However, in routine practice, diagnosis and treatment often occur as two temporally distinct stages: the former provides subtype stratification and target identification, while the latter involves systemic administration or local intervention[3,4]. Cancer is not a static entity but a dynamic system characterized by pronounced spatial heterogeneity and temporal evolution[5]. Under therapeutic selection pressure, the composition of tumor subclones, molecular profiles, and microenvironmental states continues to change[6,7]. Consequently, one-time, static diagnostic information is insufficient to support long-term therapeutic decisions[3,8], thereby limiting efficacy optimization and the realization of true individualized therapy.

In this context, theranostic platforms capable of simultaneously supporting molecular recognition, local intervention, and dynamic monitoring are emerging as a critical direction in precision cancer medicine. Theranostics, an increasingly important branch of medicine, integrates disease diagnosis with therapeutic decision-making to advance individualized healthcare[9]. Built on biomarker detection and early disease identification, this strategy tailors interventions to the patient's specific condition and provides real-time feedback or prediction of therapeutic efficacy[3,10], thereby enabling more targeted medical strategies. In this process, clinicians utilize modern imaging, genomics, and other biotechnological approaches to comprehensively evaluate disease status[11,12] and select appropriate targeted drugs or treatment modalities.

Hydrogels, three-dimensional networks formed by crosslinked hydrophilic polymer chains, possess high water content, tunable pore architectures, and mechanical properties resembling those of soft tissues. These features enable them to closely mimic the physicochemical environment of the native extracellular matrix (ECM)[13]. This not only provides a stable local environment for the retention and controlled release of bioactive components, but also allows fine control over drug diffusion, degradation behavior, and

tissue compatibility by regulating material composition, crosslinking mode, and network structure[14]. Compared with conventional systemic formulations, injectable and *in situ* gelling hydrogels can establish local drug depots through minimally invasive administration, prolong intratumoral retention, reduce off-target toxicity, and improve therapeutic precision[15]. Furthermore, hydrogel matrices can carry a wide range of functional molecules, including chemotherapeutic agents, proteins, nucleic acids, immunomodulators, exosomes, and imaging probes[14], thereby integrating diagnostic and therapeutic functions within a single material system. Their responsiveness to signals in the tumor microenvironment, such as pH, reactive oxygen species (ROS), enzymes, temperature, and light[16], further permits spatiotemporally controlled signal activation and drug release at tumor sites. Collectively, these features make hydrogels ideal materials for constructing multifunctional platforms that connect molecular recognition, targeted intervention, and real-time monitoring [Figure 1].

In recent years, the use of hydrogels in tumor diagnosis and therapeutic intervention has expanded rapidly, moving toward integrated soft-material platforms that combine biomarker recognition, intelligent release of therapeutic components, imaging-based tracking, and efficacy feedback. However, existing studies remain fragmented, and a systematic review of hydrogel-driven integrated cancer theranostic platforms is still lacking. Accordingly, this review focuses on the development and application of multifunctional hydrogels for cancer theranostics. We first systematically summarize the material matrices and crosslinking strategies used in hydrogels for tumor theranostics and clarify how structural design influences diagnostic signal generation, therapeutic payload delivery, and intelligent responsiveness. We then discuss and summarize advances since 2024 in hydrogel-based tumor molecular diagnosis, molecular therapy, and closed-loop diagnosis–treatment platforms. Finally, we examine the potential challenges and limitations of using hydrogels to construct integrated tumor theranostic platforms and highlight the prospective roles of emerging technologies, including artificial intelligence and bioelectronic interfaces, in next-generation, individualized hydrogel theranostic systems.

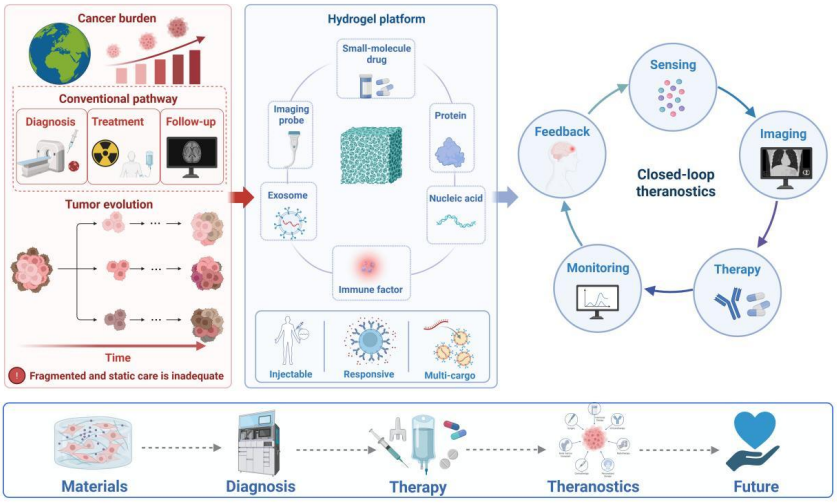


Figure 1. Schematic diagram illustrating how the hydrogel-based theranostic platform overcomes the current fragmentation between diagnosis and therapy in cancer care, thereby enabling integrated tumor diagnosis and therapy.(Figure was generated by BioRender, https://www.biorender.com/).

MATERIAL MATRICES AND FUNCTIONAL COMPONENTS OF HYDROGELS

The key to using hydrogels in integrated cancer theranostic platforms lies in their highly hydrated three-dimensional networks, which can simultaneously support biomarker enrichment, signal transduction, drug release, and efficacy monitoring[17-26]. Matrix composition determines biocompatibility and payload compatibility; crosslinking strategy governs gelation behavior and release kinetics; loaded functional components dictate recognition, imaging, and therapeutic outputs; and hydrogel network design determines whether these modules can respond on demand *in vivo* in a controllable temporal and spatial sequence[20,24-26].

Hydrogel material types and structural classification

The advantages of natural polymer hydrogels stem primarily from their ECM-mimetic properties, mild gelation conditions, and degradable chemical structures[21,27-30][Figure 2]. Alginate forms “egg-box” physical networks via divalent cations, making it suitable for encapsulating protein drugs, living cells, or nanoscale components under mild conditions. However, because it lacks mammalian enzymatically degradable sites and cell-adhesion

sequences, alginate typically requires modification through Arg-Gly-Asp (RGD) grafting, oxidative functionalization, or combination with natural ECM materials to enhance cell interactions[27-29]. Chitosan possesses a cationic backbone, mucoadhesive properties, and amino-reactive sites, enabling electrostatic complexation with negatively charged nucleic acids, exosomal membrane components, or anionic polymers. Nevertheless, its solubility, mechanical stability, and pH-dependent degradation require further regulation through polyelectrolyte complexation or dynamic covalent crosslinking[30,31]. Hyaluronic acid (HA), a representative glycosaminoglycan, combines high hydration, hyaluronidase-mediated degradability, and cluster of differentiation 44 (CD44)-mediated recognition, making it particularly valuable for tumor-targeted delivery and cell capture[32,33]. Collagen, gelatin/gelatin methacryloyl (GelMA), and silk fibroin more closely resemble proteinaceous ECM; they provide integrin recognition, matrix metalloproteinase-sensitive degradation, and tunable mechanical support, making them well-suited for constructing three-dimensional (3D) tumor models, postoperative local fillers, and delivery systems compatible with tissue repair[34-37].

Synthetic polymer hydrogels emphasize programmable structures and batch-to-batch consistency, with polyethylene glycol (PEG), polyvinyl alcohol (PVA), polyacrylamide (PAAm), and degradable block copolymers being the most common representatives[38,39]. PEG networks can regulate pore size, mechanical strength, and the release rate of encapsulated components through terminal functionalization, arm number, and crosslink density[40,41]. However, their bioinert nature necessitates the introduction of adhesive peptides, enzyme-sensitive linkers, or natural polymer segments to enable recognition by cells and the tumor microenvironment[42,43]. PVA forms stable networks through freeze–thaw cycling or chemical crosslinking and is suitable for patches, microneedles, and local covering-type delivery systems[44-47]. PAAm is commonly used in mechanically tunable *in vitro* models[48], while thermosensitive copolymers such as poly(lactic-co-glycolic acid) (PLGA)-PEG-PLGA undergo *in situ* gelation at body temperature, enabling long-acting local release[49,50].

Short or long peptides and oligonucleotides can translate their sequence information into hydrogel functionality by forming reversible networks through hydrogen bonding, π–π stacking, hydrophobic interactions, host–guest interactions, or base complementarity[51-55]. Compared with conventional polymers, these building blocks can incorporate targeting sequences, enzyme-cleavable segments, immunomodulatory motifs, or nucleic acid-recognition structures at the molecular level. Consequently, they are better suited for molecular recognition, local responsiveness, and reversible assembly[51-54]. Their primary limitation is that noncovalent networks are relatively sensitive to concentration and ionic strength; thus, they usually require combination with natural or synthetic polymers, or the introduction of secondary crosslinking, to improve structural stability *in vivo*[52-55].

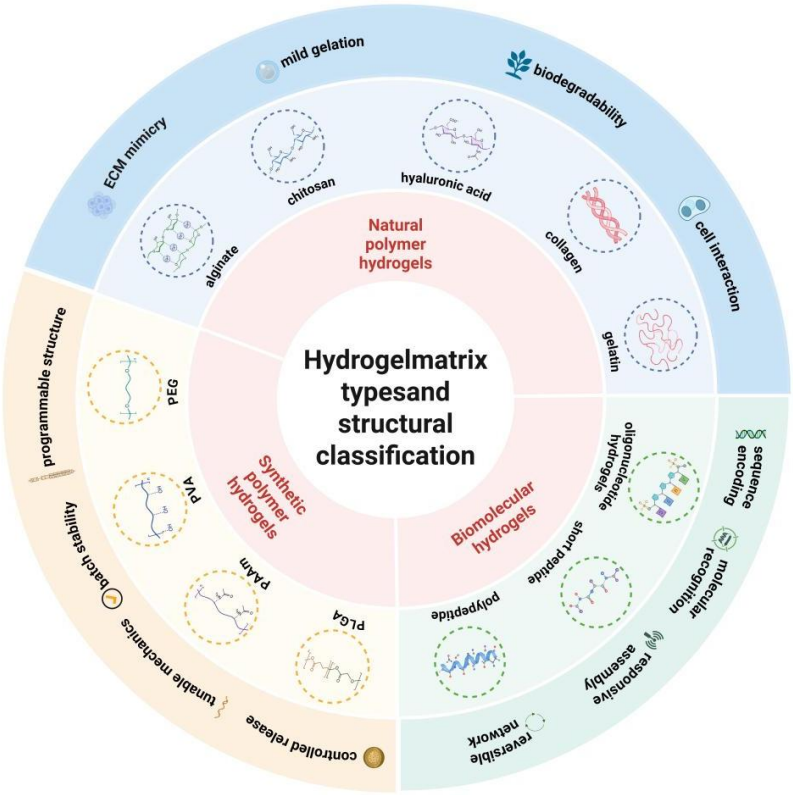


Figure 2. Schematic diagram illustrating the classification of hydrogel material components and the characteristics of hydrogels with varying matrix compositions.(Figure was generated by BioRender, https://www.biorender.com/).

Hydrogel crosslinking strategies

The crosslinking strategy dictates the transformation of a hydrogel from an injectable solution into a local network and governs the *in vivo* release profile of payloads[56,57]. Physical crosslinking relies on reversible interactions, such as ionic bonds, hydrogen bonds, and metal coordination. This approach generally offers shear-thinning behavior, self-healing capability, and minimally invasive injectability, making it suitable for applications requiring rapid spreading, local adhesion, or short- to medium-term release[58,59]. However, the gel network is highly sensitive to ionic conditions and interstitial fluid exchange. Consequently, when delivering high loads of chemotherapeutics, photosensitizers, or immune adjuvants, burst release often must be mitigated through the incorporation of nanocarriers or secondary crosslinking[60,61].

Chemical crosslinking forms relatively stable covalent networks via free-radical polymerization, photocrosslinking, click reactions, and related methods, thereby enabling precise control over gel strength, degradation rate, and payload diffusion[62]. These robust networks minimize the risks of premature material disintegration and excessively rapid drug release. Therefore, they are widely employed in postoperative cavity administration, implantable sustained-release systems, and local treatments requiring high shape fidelity[63,64]. Nevertheless, conventional small-molecule crosslinkers or initiation systems may leave toxic residues *in vivo*. Furthermore, crosslinking processes involving free radicals or other highly reactive agents may compromise the bioactivity of loaded therapeutics[65,66].

Dynamic covalent crosslinking combines chemical stability with reversible responsiveness, allowing bond exchange or cleavage under stimuli such as pH, redox conditions, or glucose. This makes it suitable for constructing adaptive release systems, tissue-adhesive materials, and degradable networks[67]. However, because dynamic covalent bonds are intrinsically reversible, hydrogel networks in body fluids may be influenced by pH, redox state, and reaction conditions, leading to fluctuations in gelation efficiency, network strength, and drug-release behavior[68]. In practice, optimizing crosslink density, bond-exchange kinetics, and local delivery conditions is often necessary to balance responsiveness and durability[68].

Biological crosslinking primarily involves constructing hydrogel networks under mild, physiologically compatible conditions by harnessing catalytic or recognition mechanisms derived from biological systems.Compared with traditional chemical crosslinking, these strategies can usually be conducted at physiological pH and temperature without ultraviolet irradiation or highly reactive crosslinkers, and are therefore more conducive to preserving the functional integrity of active components, such as cells, proteins, and nucleic acids, during gelation[69-70]. Beyond classical enzyme-mediated crosslinking, biomolecular recognition systems based on DNA base pairing or aptamer–target recognition are often regarded as functional extensions of biological crosslinking[71,72]. A defining feature of such systems is that the crosslinking units not only participate in network formation but also mediate molecular recognition, signal response, and payload regulation, thereby facilitating integration with tumor diagnostic applications[73]. However, the gelation efficiency and final network properties of these hydrogels often depend on enzyme activity, substrate structure, and the local microenvironment. Consequently, gelation speed, crosslink density, and mechanical performance may fluctuate across material batches or in complex body-fluid environments[69,70].

Multifunctional hydrogels with composite architectures

In hydrogel-mediated cancer theranostic design, the matrix composition and crosslinking strategy together determine the hydrogel's recognition of tumor-associated signals, responsiveness, and therapeutic outputs. Natural polysaccharide or protein matrices mimic the ECM, offering tissue adhesion and enzymatic degradability, which facilitates the immobilization of cells, vesicles, nucleic acid probes, or protein factors. Conversely, synthetic networks such as PEG and PVA ensure stable local retention and act as diffusion barriers through the regulation of terminal reactions, crosslinking density, and pore size[27,28,38-40]. Integrating distinct matrices into composite networks via diverse crosslinking mechanisms allows hydrogels to maintain structural stability while generating controllable responses to the tumor microenvironment or exogenous stimuli, thereby rendering both gelation and cargo release tunable[56-58,67-68].

Nanogels are hydrogel structures with crosslinked networks reduced to the nanoscale. They retain the high water content and swelling properties of bulk hydrogels while exhibiting the favorable diffusibility, ease of modification, and responsive controllability characteristic of nanocarriers[74,75]. Compared with bulk hydrogels, nanogels diffuse more readily through blood or the tumor interstitium and can be engineered to recognize biomarkers via antibodies, aptamers, or peptide ligands[76]. Their network structures respond to the tumor microenvironment or external stimuli, translating material-level structural changes into signal enhancement or payload release[75,77-79]. In diagnostics, nanogels serve as microreactors or signal-enrichment units to increase the local concentration of low-abundance biomarkers. In therapy, they function as drug reservoirs embedded within bulk hydrogels; the bulk gel ensures lesion retention, while the nanogels mediate tissue penetration, cellular uptake, and microenvironment-triggered release[76-79].

Liposome–hydrogel composite systems combine the drug-loading capacity of liposomes with the local retention and sustained-release properties of hydrogels[80]. Lipid bilayers encapsulate drugs or functional molecules, improving payload stability and delivery compatibility, whereas hydrogel networks restrict diffusion at injection or implantation sites, reduce premature leakage, and prolong local exposure[81-83]. By tuning pore size, crosslink density, and degradable linkages, liposome release, drug extravasation, and gel degradation can be coordinated across different timescales[82]; with the further introduction of stimulus-responsive modules, synergistic triggering by exogenous stimuli and the tumor microenvironment can also be achieved[84]. Metal–drug coordination networks, two-dimensional nanomaterials, and carbon-based nanostructures can also be embedded within hydrogels to provide metal-ion imaging, catalytic therapy, photothermal conversion, or electrical/acoustic responsiveness. However, risks related to metal accumulation, long-term degradation, nanomaterial migration, and local inflammation must be evaluated concurrently[85-87].

APPLICATIONS OF HYDROGELS IN TUMOR DIAGNOSIS

Biosensing and molecular biomarker recognition

In recent years, the role of hydrogels in tumor diagnosis has evolved from passive carriers to diagnostic platforms that integrate sample enrichment, activity preservation, controlled release, and signal amplification. This evolution is particularly evident in liquid biopsy, where biomarkers such as circulating tumor cells (CTCs), circulating tumor DNA (ctDNA), microRNAs (miRNAs), and exosomes/extracellular vesicles (EVs) are typically dispersed in complex matrices such as blood, urine, saliva, or tissue fluid, and are generally characterized by low abundance, strong heterogeneity, susceptibility to interference from background components, and, for some molecules, poor stability[88-90]. Owing to their highly hydrated three-dimensional networks and tissue-like softness, hydrogels can provide a gentler microenvironment for the capture of cells, vesicles, and nucleic acids[91]. At the same time, recognition modules such as antibodies, aptamers, and nucleic acid probes can be introduced into the network to enable selective enrichment of target biomarkers[92-93]. More importantly, the pore architecture, swelling/shrinking behavior, and degradability or stimulus responsiveness of hydrogels can also support biomarker release and signal amplification when needed[94-97][Figure 3]. Lu and colleagues[98] proposed stimulus-responsive signal-amplifying hydrogel microparticles termed Novabeads. In this system, poly(ethylene glycol) diacrylate (PEGDA) served as the network matrix, and pH-responsive acrylic acid motifs were incorporated, resulting in approximately 5-fold volumetric contraction under pH regulation. Coupled with high-density bioreceptor loading, this contraction effect markedly enhanced fluorescence signals and enabled enzyme-free detection of the cancer-associated miR-16. Compared with conventional hydrogel microparticles, this platform achieved more than a 30-fold signal enhancement and a substantially lower limit of detection, demonstrating that the hydrogel itself can function directly as a signal-amplifying element in the diagnostic process.

CTCs are important liquid-biopsy biomarkers for monitoring metastasis and recurrence, yet they are extremely rare in peripheral blood, and distinct CTC subpopulations exhibit pronounced heterogeneity in epithelial–mesenchymal plasticity (EMP) and stemness-related phenotypes/marker expression[99-100]. Accordingly, the frontier of hydrogel-based CTC capture platforms has shifted from simply increasing capture numbers to emphasizing heterogeneous biomarker recognition, cell viability preservation, and subsequent release-

based analysis. In the context of heterogeneous biomarker recognition, one study developed a CXCL12-loaded HA hydrogel (CLG) to capture metastasis-prone CTCs[101]. This system exploits the chemokine (C-X-C motif) ligand 12/C-X-C chemokine receptor type 4 (CXCL12/CXCR4) axis to attract invasive CXCR4-positive cells into the hydrogel network. Compared with conventional hydrogel platforms that rely on epithelial cell adhesion molecule (EpCAM), this strategy is less constrained by EpCAM downregulation during epithelial–mesenchymal transition (EMT). It preferentially enriches CTC subpopulations with hybrid epithelial–mesenchymal phenotypes, stem cell-related features, and invasive metastatic potential, thereby providing a basis for metastasis risk assessment and downstream phenotypic analysis. With respect to preserving cell viability for downstream analysis, another representative advance is a bis-histidine-mediated cell-imprinted hydrogel for the precise capture and dynamic release of circulating hepatocellular carcinoma cells[102]. This system improves recognition of target tumor cells through the combined use of sialylated glycans (SGs) and cell-imprinted morphology. Specifically, L-histidine-L-histidine (HH) was integrated into a low-swelling poly(ethylene glycol) dimethacrylate (PEGDMA) cell-imprinted hydrogel to generate imprinted sites on the material surface that closely match the size and contour of the target cells, thereby coupling molecular-scale affinity recognition with cell-scale spatial matching. Because the interaction between HH and SGs is tunable, intact release of captured CTCs can be achieved under the mildly alkaline conditions of trypsin–ethylenediaminetetraacetic acid (trypsin-EDTA), while preserving membrane integrity, proliferative capacity, and subsequent passaging potential to the greatest extent possible.

Compared with CTCs, ctDNA is better suited to reflecting mutational spectra, minimal residual disease, and the evolution of therapeutic resistance, but its short fragment length and low abundance, together with dilution by large amounts of normal cell-free DNA (cfDNA), pose major analytical challenges[103-104]. Current hydrogel platforms are therefore evolving not only toward higher-efficiency ctDNA enrichment but also toward programmable structures and integrated signal transduction. A notable example has already demonstrated, in breast cancer, the coupling of target ctDNA recognition, material structural transformation, and signal output within a single homogeneous reaction, breaking

away from the conventional workflow of hydrogel capture, washing/sorting, and subsequent polymerase chain reaction (PCR) or instrument-based amplification readout [105]. In that study, a rolling circle amplification (RCA)-derived DNA hydrogel was integrated with DNA@Cu^{2+} nanospheres to simultaneously analyze two hotspot mutations in breast cancer, PIK3CA and ESR1, within a single system. Upon ctDNA recognition, the DNA hydrogel actively disassembles to expose a G-quadruplex structure that generates a thioflavin T (ThT) turn-on signal; simultaneously, the nanomaterial releases Cu^{2+}, causing a quantum-dot turn-off. Target recognition is thus converted into dual orthogonal signal outputs through hydrogel disassembly and nanosphere decomposition, reducing sample loss and improving the detection efficiency of low-abundance ctDNA. DNA methylation analysis represents another frontier in ctDNA-based liquid biopsy. Hou and colleagues constructed a thermosensitive hydrogel-enhanced one-pot recombinase polymerase amplification (RPA)-CRISPR/Cas12a system[106], combined with methylation-sensitive restriction endonucleases, for the ultrasensitive detection of specific methylation sites in breast cancer ctDNA. By employing a thermosensitive hydrogel, this method achieved spatial separation while maintaining reaction connectivity within a single tube for the first time, thereby alleviating target depletion and reduced sensitivity caused by premature Cas12a cleavage. Thus, hydrogels no longer function merely as reaction vessels but as integrated reaction systems capable of regulating amplification, nuclease digestion, and signal readout through spatial organization.

Current quantitative techniques for multiple miRNAs typically require RNA extraction from body fluids as a preprocessing step[107]. This process is labor-intensive and may compromise analytical accuracy due to target miRNA loss and degradation[108]. There is therefore a pressing need for reaction systems that can directly process body fluids without preprocessing. Recently reported size-coded PEG hydrogel bead systems have advanced hydrogel platforms toward extraction-free, multiplex miRNA liquid biopsy analysis in real serum samples[109-112]. In one study, capture probes for miR-21, miR-205, and miR-375 were immobilized in beads of different diameters, allowing target miRNAs to diffuse directly from serum into the beads without RNA extraction and to be selectively retained. RCA amplification was then completed within the beads, and parallel quantification of the

three miRNAs was achieved by size-based grouping via flow cytometry; when combined with machine-learning analysis, this strategy enabled lung cancer diagnosis and subtype classification[110]. This also reflects the broader shift of liquid biopsy toward automation, multiparametric measurement, and algorithm-assisted diagnosis.

Resolving the heterogeneity of extracellular vesicles and particles (EVPs) derived from single cells is of major importance for elucidating mechanisms of tumor metastasis and advancing cancer medicine[113]. Existing single-cell EVP microfluidic systems generally struggle to simultaneously achieve source purity and long-term culture[114-115], and technologies capable of independently isolating and sealing single cells along with their secreted EVPs over extended culture periods remain lacking. The emergence of a microwell array composed of oil-sealed, RGD-modified alginate hydrogel has helped address this gap[116]. By integrating oil-sealed isolation with RGD-modified alginate hydrogel microwells, this study established a gel system capable of simultaneously achieving independent single-cell confinement and *in situ* retention of secreted EVPs during long-term culture. The oil layer isolates each microwell from the others, preventing inter-well mixing of EVPs; the size-selective permeability of the alginate hydrogel mesh allows nutrients and soluble factors to pass while blocking EVP escape; and the RGD motif provides adhesion sites for adherent cells, with culture medium continuously replenished through a polydimethylsiloxane (PDMS) spacer layer at the base. This platform provides a foundation for future liquid biopsy studies in which single-cell-derived EVs can be traced to their source.

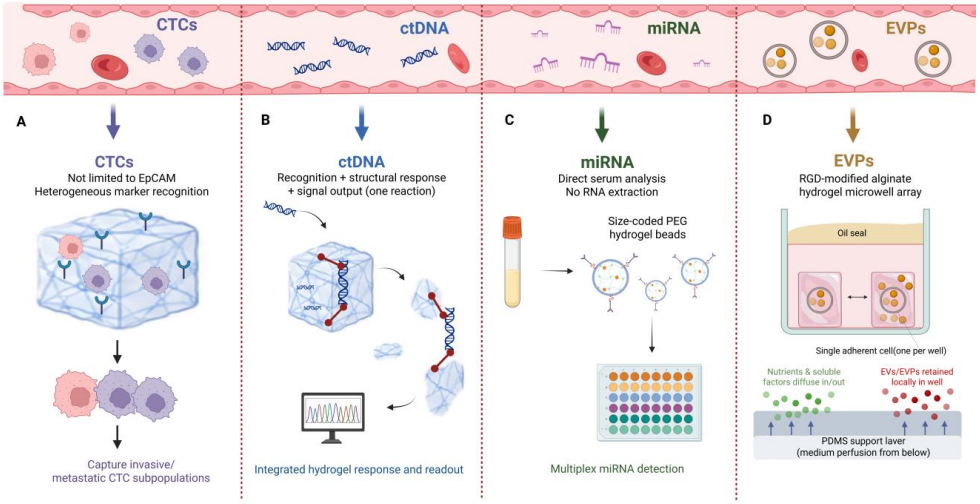


Figure 3. Schematic diagram illustrating capture methods for different liquid biopsy biomarkers. (A) Current CTC capture methods are no longer limited by the heterogeneity caused by EpCAM downregulation; (B) Recognition of target ctDNA, structural changes of the material, and signal output have been achieved within a hydrogel platform; (C) Using a size-encoded PEG hydrogel microbead system, extraction-free multiplex miRNA liquid biopsy analysis can be performed in authentic serum samples; (D) By integrating oil-sealed isolation with hydrogel microwells, single cells and their secreted EVPs can be independently isolated and confined during extended culture periods.(Figure was generated by BioRender, https://www.biorender.com/)

Visual imaging and image guidance

Because of their hydrated three-dimensional network structure, hydrogels can locally confine imaging probes, reduce premature probe leakage, and protect signal-generating components from rapid inactivation or nonspecific diffusion, making them highly important imaging matrices in tumor diagnosis[117-119]. Compared with freely diffusing small-molecule probes or nanoparticles, hydrogel-based systems generally exhibit longer retention at tumor sites or in postoperative cavities and more readily couple signal generation to endogenous cues, such as adenosine triphosphate (ATP), pH, and enzymes, or to externally applied optical stimulation[120-121]. Consequently, hydrogels have evolved from passive contrast agent carriers into programmable materials for lesion localization, intelligent response, and therapeutic monitoring and prediction [Figure 4].

Fluorescence imaging remains one of the most accessible diagnostic modalities due to its high sensitivity, operational simplicity, and compatibility with intraoperative visualization[122]. However, the diagnostic utility of conventional fluorescent probes is often limited by rapid diffusion, photobleaching, aggregation-caused quenching, and insufficient retention at lesion sites[123,124]. Hydrogel encapsulation partially addresses these limitations by providing a hydrated microenvironment that stabilizes organic fluorescent dyes, aggregation-induced emission nanoparticles, and other luminophores[125,126]. In 2013, Jungmin Park and colleagues developed a near-infrared-sensitive molecular imaging probe based on a hydrogel composite[127]. In this system, HA served as the matrix, conferring CD44-targeting capability, while a near-infrared-sensitive organic dye was encapsulated. Upon near-infrared excitation, the hydrogel emitted fluorescence, enabling the imaging of gastric cancer cells expressing CD44. From the standpoint of current frontier research, the development of fluorescence-optical imaging hydrogels has shifted from early systems that relied on single-cell surface receptor recognition to highly sensitive, stimulus-responsive tumor molecular imaging platforms. Yang and colleagues further constructed a tumor microenvironment-responsive DNA hybrid hydrogel, termed AHB Gel[128]. By coupling a PAAm hydrogel network with an ATP-responsive aptamer, this system can directly sense abnormally elevated extracellular ATP levels in the tumor microenvironment while maintaining close tissue contact without tissue invasion. It rapidly activates fluorescence under high-ATP conditions but produces almost no obvious fluorescence against the low-ATP background of normal tissues. As a result, this hydrogel not only enables highly selective recognition of tumor tissue but also creates a clear boundary between tumor and normal tissue, thereby improving the accuracy of lesion localization and margin delineation. On this basis, further integrating responsive fluorescent probes into hydrogel systems that can be locally coated or formed *in situ* can establish a transiently stable imaging interface within the surgical cavity for intraoperative navigation and residual-disease detection. Walker and colleagues developed a locally spreadable thermosensitive imaging gel in which AKRO-QC-ICG was loaded into a Pluronic F-127 matrix for the rapid identification of residual breast cancer tissue within surgical cavities[129]. After local tissue contact, this gel generated sufficient fluorescence contrast within 10 min to distinguish the tumor from

the surrounding normal tissue, and high signal-to-noise ratios were retained even after washing. In both murine orthotopic models and patient-derived xenograft (PDX) models, it demonstrated high sensitivity and specificity for lesion detection. For cancers with highly heterogeneous molecular markers, the recent emergence of fluorescent gels targeting tumor-microenvironment components offers a new solution[130]. Their design no longer relies primarily on highly heterogeneous tumor-cell surface molecules but instead shifts toward using relatively stable collagen components in the tumor microenvironment as anchoring sites. This study showed that collagen-adhesive probes can improve the sensitivity and stability of intraoperative fluorescence imaging for bladder cancer, thereby providing a new imaging strategy for lesions such as non-muscle-invasive bladder cancer (NMIBC), in which accurate boundary delineation is particularly critical.

Beyond intraoperative residual disease detection, hydrogel fluorescence imaging platforms are increasingly applied to the localization of deep lesions during endoscope-assisted or minimally invasive procedures. Near-infrared fluorescence imaging offers deeper tissue penetration, lower autofluorescence, and greater suitability for solid tumors located in complex or relatively deep anatomical regions. Accurate localization of deep lesions remains a major challenge in endoscope-assisted minimally invasive surgery. The team of Seon[131] developed a thermosensitive hydrogel loaded with near-infrared dyes that can safely, durably, and visibly localize deep lesions in real time during endoscopic surgery. In this system, indocyanine green (ICG) or ICG-human serum albumin (HSA) was incorporated into a thermosensitive hydrogel. Because the material remains fluid at low temperatures but undergoes a sol–gel transition at physiological temperatures after *in vivo* administration, it can gel *in situ* after local injection into a lesion, thereby confining the dye locally and reducing its diffusion into surrounding tissues. This provides a more stable preoperative-to-intraoperative imaging reference for sustained localization of deep lesions and fluorescence-guided minimally invasive surgery.

Unlike near-infrared fluorescence imaging, which is mainly used for spatial localization, second near-infrared window (NIR-II) photoacoustic imaging emphasizes converting differences in optical absorption within tumor tissues into acoustic signals that can be

detected at depth[132], and is therefore better suited for coupling with tumor-microenvironment parameters such as pH, temperature, or metabolic state [133,134]. Conventional always-on photoacoustic probes, however, continuously emit signals in normal tissues, making them susceptible to interference from endogenous chromophores such as hemoglobin and thereby limiting lesion specificity. To address this, Sun and colleagues[133] constructed a low-pH-triggered, thermal-responsive volume phase-transition nanogel, gold nanorod@poly(N-isopropylacrylamide)-vinyl acetic acid (AuNR@PNIPAM-VAA). Gold nanorods (AuNRs) provide photothermal conversion and generate photoacoustic signals, whereas the PNIPAM-VAA shell acquires low-pH-dependent thermoresponsive volume-phase transition behavior through the introduction of vinyl acetic acid. Following laser irradiation, AuNRs convert light into heat and raise the local temperature; because tumor regions generally exhibit lower pH than normal tissues, the shell undergoes a swelling-to-collapse phase transition specifically within the tumor. During this process, the local refractive index around the AuNRs increases, the longitudinal plasmon resonance red-shifts, and the NIR-II photoacoustic signal is substantially amplified. Furthermore, Jeff and colleagues[135] constructed tumor-targeted PAAm hydrogel nanoparticles in combination with photoacoustic chemical imaging to predict the chemotherapeutic response of breast cancer by monitoring pH changes in the tumor microenvironment. Their group embedded the pH-sensitive dye seminaphthorhodafluor-5/6F (SNARF-5/6F) into the hydrogel and generated quantitative pH maps using multiwavelength ratiometric photoacoustic chemical imaging, thereby monitoring tumor-microenvironment pH in patient-derived breast cancer xenografts during alkalinization therapy and chemotherapy to achieve efficacy monitoring and prediction.

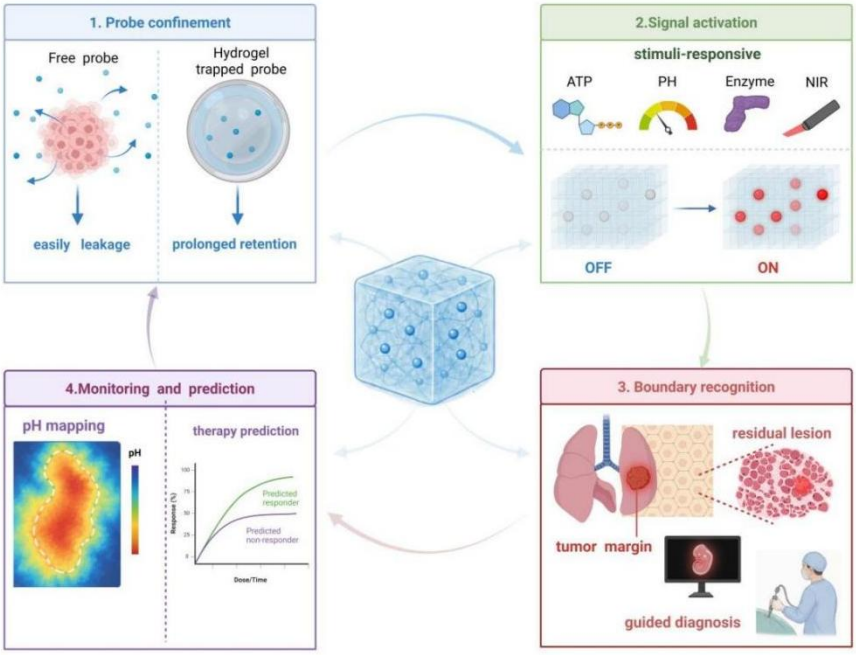


Figure 4. Schematic diagram of hydrogel-based tumor visualization imaging and image-guided modalities. The hydrogel network confines the retention of imaging components and can integrate with the tumor microenvironment to confer smart responsive properties, enabling tumor visualization and the reflection or prediction of therapeutic outcomes.(Figure was generated by BioRender, https://www.biorender.com/).

APPLICATIONS FOR HYDROGELS IN TUMOR THERAPY

In therapeutic settings, hydrogels place greater emphasis on actively regulating local tumor pharmacokinetics, the spatiotemporal distribution of different treatment modalities, and the post-treatment microenvironment[136-140]. Leveraging their highly hydrated three-dimensional networks, injectable *in situ* gelation, tunable crosslink densities, and stimulus responsiveness, hydrogels can not only serve as sustained-release depots that prolong the retention of therapeutic agents within tumors or postoperative cavities[136], but can also integrate chemotherapy, immunomodulation, and photo-, sono-, and magnetically mediated therapies to reduce systemic exposure and enhance local treatment intensity[137,139,140]. Hydrogels are therefore now widely used throughout the course of cancer therapy [Figure 5].

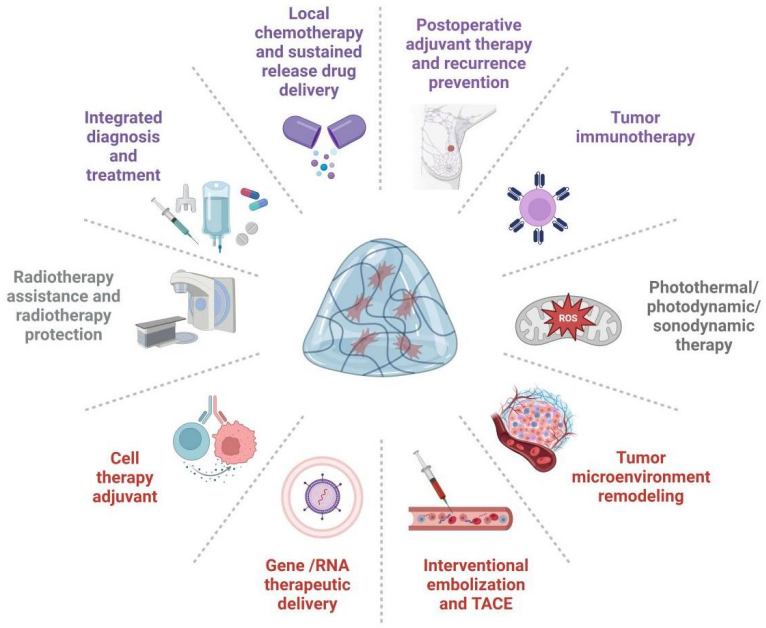


Figure 5. Schematic summary of current application strategies of hydrogels in tumor therapy.(Figure was generated by BioRender, https://www.biorender.com/).

Chemotherapeutic drug delivery

Chemotherapy remains an essential component of treatment for many solid tumors, but small-molecule chemotherapeutics often face problems such as nonspecific distribution, fluctuations in plasma concentration, insufficient intratumoral retention, and dose-limiting toxicity[141]. The core value of hydrogel-based delivery systems lies in changing the mode of drug exposure: through local injection, postoperative cavity filling, mucoadhesion, or transdermal delivery, hydrogels can transform transient systemic peak concentrations into sustained and relatively stable drug release at the tumor site, and can further achieve tumor microenvironment (TME)-responsive release by exploiting differences in pH, enzyme activity, redox status, or temperature[136,137,142-144].

Exhibit well-established broad-spectrum antitumor activity, but their clinical utility is limited by cardiotoxicity, myelosuppression, and the risk of resistance[141]. One study developed an injectable pH-responsive polypeptide hydrogel, FOK, for the local sustained release of DOX[142]. This system maintains a stable gel structure at physiological pH but

degrades gradually in the acidic tumor environment, thereby promoting DOX release and prolonging its therapeutic effect at the tumor site. Compared with free DOX, the DOX/FOK hydrogel better maintains effective local cytotoxic concentrations by reducing premature drug diffusion and systemic exposure. Shi and colleagues[143] further reported an HA-based injectable DOX-loaded hydrogel, DOX-MCHAgel, for locoregional breast cancer therapy and metastasis inhibition. In a 4T1 breast cancer model, this hydrogel achieved sustained DOX release for more than 10 d and significantly suppressed primary tumor growth as well as liver and lung metastases, without evident systemic toxicity. These findings indicate that the therapeutic value of hydrogels lies not only in the local sustained release of chemotherapeutic drugs, but also in confining drug exposure to tumors and adjacent high-risk areas, thereby reducing distal organ toxicity and diminishing opportunities for metastatic dissemination. For solid tumors with a high risk of postoperative recurrence, hydrogels can also function as local therapeutic depots within postoperative cavities to eliminate residual tumor cells and improve the tissue-repair microenvironment. Zhang and colleagues developed a composite system, ZC-DOX@GEL, in which a GelMA hydrogel was loaded with DOX@zeolitic imidazolate framework-8 (ZIF-8)/cerium dioxide (CeO_2) nanoparticles for postoperative tumor treatment and wound repair[144]. In this platform, ZIF-8 serves as a DOX nanocarrier to improve drug loading and acid-responsive release, whereas CeO_2 nanoparticles alleviate postoperative local oxidative stress and promote wound healing; the GelMA network further immobilizes the nanoparticles within the postoperative cavity, endowing the system with residual tumor eradication, controlled drug release, and tissue-repair functions.

In superficial lesions, such as skin tumors, hydrogel microneedles (HMNs) offer a new structural platform for the local delivery of chemotherapeutic agents or combination therapeutics. HMNs can penetrate the stratum corneum and form continuous hydrogel microchannels, thereby overcoming the skin-barrier limitation of conventional transdermal delivery while being better suited than standard injections for localized, repeatable, and minimally invasive administration[145]. As part of transdermal drug delivery systems (TDDS), microneedles perforate the epidermis and create microchannels; because of their hydrophilicity, they swell to form continuous hydrogel conduits[146,147]. These channels

facilitate drug diffusion and ensure stable and sustained therapeutic effects. HMNs have now evolved into integrated drug-delivery systems capable of loading multiple drugs or immune adjuvants for combination cancer therapy. Zhang and colleagues[148] constructed a bifunctional HA-based HMN system in which the needle tips were loaded with CCa@TF/chlorin e6 (Ce6) nanocomposites and rapidly dissolved after insertion into tumors to release therapeutic components. The hydrogel base, HB-PVA, formed via boronate ester bonds between 3-aminophenylboronic acid-grafted HA and PVA, remained locally to support subsequent skin repair. During treatment, CCa@TF/Ce6 mediated photothermal therapy (PTT) and photodynamic therapy (PDT), respectively, under dual-laser irradiation. More importantly, ROS and thermal stimulation also induced immunogenic cell death (ICD), promoted dendritic cell (DC) maturation, and drove macrophage polarization from the M2 to the M1 phenotype, thereby converting local physical/oxidative injury into antitumor immune activation.

In urologic malignancies, hydrogel delivery systems can also address the problem of intracavitary drug clearance caused by continuous urine dilution, periodic bladder emptying, and insufficient mucosal retention. After surgery for NMIBC, intravesical instillation is often limited by urine dilution, voiding, and poor mucosal retention, resulting in insufficient effective drug-contact time[149]. Mucoadhesive or reverse thermosensitive hydrogels can be instilled as liquids at low temperature and form local drug depots after entering the bladder at body temperature, thereby prolonging the contact of chemotherapeutic agents with urothelial tumor tissue. Zheng and colleagues proposed an adhesion-to-penetration-transformable nanomotors-in-hydrogel system for intravesical therapy[150], combining the intracavitary retention of conventional hydrogels with the active penetration capability of nanomotors. This platform used poloxamer 407 (PLX), HA, and sodium bicarbonate to construct a self-disintegrating composite hydrogel. PLGA nanoparticles loaded with gemcitabine (Gem) were coated with bladder cancer cell membranes and conjugated with urease to form urease-powered membrane nanomotors (UMN), which were then encapsulated within the hydrogel network. After intravesical instillation, the PLX hydrogel underwent *in situ* gelation at body temperature and adhered to the urothelial surface, thereby prolonging GEM retention in the bladder lumen and

enriching UMN at the mucosal surface. Subsequently, urea in urine diffused into the hydrogel, creating a concentration gradient. The UMN acquired motility by catalyzing urea, allowing them to migrate directionally along the gradient and actively traverse the urinary mucus layer and the dense urothelial barrier, thereby delivering GEM into deeper bladder tissues [Figure 6].

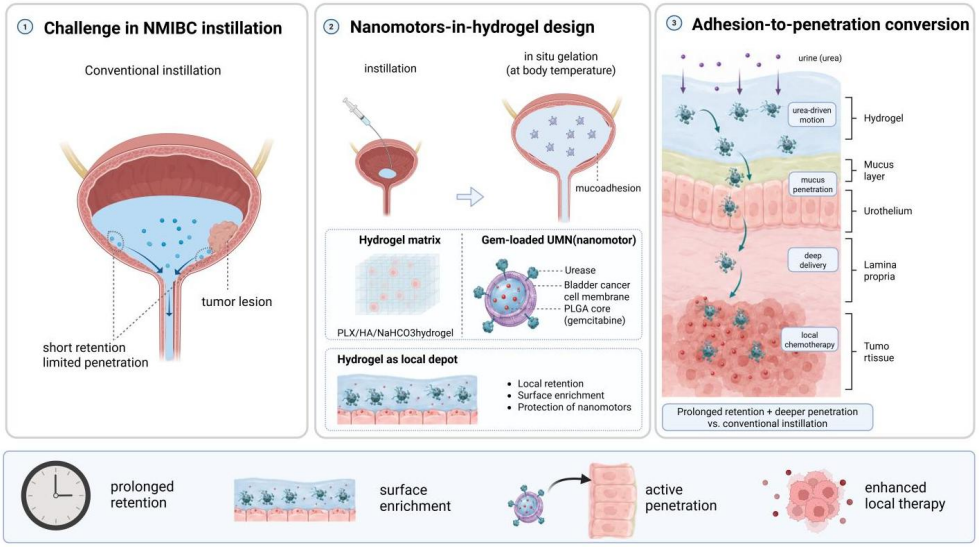


Figure 6. Schematic diagram illustrating the combination of hydrogels and nanomotors for mitigating intravesical drug clearance during intravesical administration. ① Conventional intravesical drug delivery is susceptible to urine flushing, leading to poor therapeutic efficacy; ② Drug-loaded hydrogels enable favorable intravesical retention of therapeutic components; ③ Nanomotors embedded within the hydrogel can actively migrate, achieving better penetration capability.(Figure was generated by BioRender, https://www.biorender.com/).

Cancer vaccine carriers

With the continued evolution of vaccine technologies, cancer vaccines can now be designed for patients with established malignancies to induce tumor-specific immune activation and thereby promote targeted recognition and clearance of tumor cells[151,152]. Nevertheless, the development of effective cancer vaccines still faces many challenges. For example, insufficient release of tumor antigens by tumor cells can limit antigen uptake by immune

cells. Inadequate antigen processing by antigen-presenting cells restricts the generation of antigen-specific T-cell responses[153]. In addition, the immunosuppressive tumor microenvironment can lead to effector-cell exhaustion and death[154]. Rationally designed delivery technologies, including lipid nanoparticles, hydrogels, scaffolds, and polymeric nanoparticles, can target therapeutic agents to tumor cells, immune cells, or the ECM and thereby effectively overcome these challenges[155-158]. In cancer therapy, hydrogels hold particular promise for maximizing the efficacy of cancer vaccines. On the one hand, the highly porous network structure of hydrogels can protect vaccines from *in vivo* degradation; on the other hand, hydrogels enable not only minimally invasive injection near the tumor site, but also spatiotemporally controlled release of vaccine formulations[155,156].

In situ tumor vaccines represent one of the most characteristic directions in hydrogel vaccine systems. Their basic concept is that individualized antigens released after local tumor-cell death are recognized by the immune system *in situ*. Because postoperative tumor-injury regions are often accompanied by bleeding and tissue-fluid exudation, conventional *in situ* vaccines are readily diluted, displaced, or lost, leading to insufficient local drug exposure. Qiu and colleagues reported a rapidly hemostatic *in situ* hydrogel tumor vaccine for chemotherapy-immunotherapy in colorectal cancer[159]. This system can rapidly achieve hemostasis and local retention at tumor-resection or injury sites while continuously releasing oxaliplatin to induce ICD in tumor cells and stimulate the release of individualized antigens, thereby locally amplifying the antigen source and activating antitumor immunity. *In vivo* experiments showed that it not only suppressed the growth of orthotopic colorectal cancer but also inhibited distant untreated tumors. The modular hydrogel vaccine proposed by Ji and colleagues further illustrates the logic of spatiotemporally ordered release desig[160]. In this system, chemokine (C-C motif) ligand 21a (CCL21a) and tumor-cell-derived exosomes loaded with granulocyte-macrophage colony-stimulating factor (GM-CSF) messenger RNA and Ce6 were co-assembled into a nanoclay/GelMA hydrogel. CCL21a was released earlier to guide metastatic cells from tumor-draining lymph nodes into the hydrogel, whereas subsequently produced GM-CSF continuously recruited and activated DCs; after sonodynamic therapy killed trapped tumor

cells, the dead cells within the gel themselves became an antigen source, ultimately forming a closed-loop immune process.

With the development of antigen screening and immune checkpoint blockade (ICB) therapy, hydrogel vaccines are also moving toward defined antigens and combination ICB strategies. Hepatocellular carcinoma itself elicits relatively weak immune responses, and ICB alone is often insufficient to fully activate antitumor T cells. Zhao and colleagues used transcriptomic analysis to identify kinesin family member 20A (KIF20A) as an overexpressed antigen in hepatocellular carcinoma and then constructed a KIF20A protein/resiquimod (R848) liposome-loaded thermosensitive PLGA-PEG-PLGA hydrogel vaccine, K/RLip@Gel[161]. This hydrogel forms a sustained local depot for antigen and adjuvant release, enhances DC maturation and T-cell infiltration, and improves the therapeutic efficacy of anti-programmed death-ligand 1 (anti-PD-L1) treatment in subcutaneous, orthotopic, and immune-humanized PDX models of liver cancer. Wang and colleagues, by contrast, developed an injectable thermosensitive oncolytic hydrogel, LC-Gel, for the co-delivery of the oncolytic peptide LTX-315 and the chemokine CCL21 to tumor sites[162]. LTX-315 induces tumor-cell ICD and exposes antigens, whereas the sustained release of CCL21 recruits DCs to capture these antigens and thereby promotes T-cell activation. In an orthotopic breast cancer model, this system inhibited tumor growth while inducing long-term immune memory and distant antitumor effects.

Hydrogel-based three-dimensional tumor models and drug screening

The role of hydrogels in cancer therapy is not limited to *in vivo* drug-delivery systems but also extends to the *in vitro* construction of 3D tumor models for the discovery, screening, and optimization of therapeutic strategies. Conventional two-dimensional (2D) culture cannot recapitulate tumor 3D architecture, cell–ECM interactions, or oxygen/nutrient gradients, and its drug-response profiles therefore often deviate from *in vivo* efficacy[163-164]. Although PDX models are closer to clinical reality, they are time-consuming and costly and cannot readily satisfy high-throughput screening demands[165]. Compared with traditional animal-derived matrices such as Matrigel, recent research has increasingly emphasized hydrogel systems with chemically defined composition, tunable mechanical properties, and

intrinsic bioactivity[166-169]. Hydrogels modulate ECM signals through diverse material matrices and simulate tissue- or stage-specific stiffness by adjusting crosslinking density[170-171]. Stiffness modulation is particularly critical for tumors such as pancreatic cancer, where extensive fibrosis and matrix stiffness significantly influence therapeutic response[172]. One study developed a synthetic hydrogel based on sodium alginate (NaA) and HA for pancreatic cancer organoid culture and drug testing[173]. By tuning hydrogel stiffness, this model mimicked the pancreatic cancer stromal environment, demonstrating that biomimetic stiffness enhanced resistance to conventional chemotherapeutics while increasing the sensitivity of epidermal growth factor receptor (EGFR)-mutant organoids to erlotinib. Furthermore, hydrogel-based 3D tumor models have been employed to reconstruct invasive phenotypes in breast cancer and evaluate drug responses in colorectal cancer, thereby supporting subsequent individualized screening[174,175].

Hydrogel-based 3D models encapsulate patient-derived tumor cells within a controllable tumor microenvironment, enabling the construction of patient-derived organoid (PDO) systems. By tuning the mechanical strength, chemical composition, and bioactive ligands of hydrogels, researchers can more closely recapitulate ECM states across different tissues or tumor types[176-177].Regarding co-culture with stromal components, Luo and colleagues previously developed an HA-gelatin hydrogel-based co-culture model of colorectal cancer (CRC) PDOs and cancer-associated fibroblasts (CAFs)[178]. In this system, CRC PDOs were embedded in an HA-gelatin hydrogel and co-cultured with patient-derived CAFs, thereby better preserving the molecular features of primary tumors and tumor–stroma interactions for the evaluation of standard chemotherapeutic drugs. More recently, Zhao and colleagues developed HADR, a chemically defined, mechanically tunable, and bioactive HA/alginate double-network hydrogel for hepatocellular carcinoma organoid construction[179]. This system comprises methacrylated HA, sodium alginate, methacrylamide dopamine, and c(RGDFC); its stiffness can be regulated to approximate physiological liver tissue while supporting the formation of hepatocellular carcinoma organoids in a 3D environment. Compared with 2D culture, HepG2 organoids grown in HADR exhibited a higher half-

maximal inhibitory concentration for DOX, indicating that a 3D ECM-like environment more faithfully reflects *in vivo* drug tolerance.

Hydrogel-based 3D models also facilitate high-throughput drug screening, promoting individualized drug selection and accelerating precision medicine across diverse tumor types. Jung and colleagues combined engineered ECM-mimetic hydrogels with high-throughput 3D bioprinting to construct 3D models of patient-derived neuroblastoma and sarcoma[180]. This platform rapidly generates multiwell-format 3D tumor models from limited patient samples while preserving the genetic and phenotypic features of primary tumors, thereby enabling individualized drug-sensitivity analysis. Miebach and colleagues proposed an *in vitro* 3D hydrogel-based tumor-resection model in which pancreatic cancer cells were used to create standardized resection cavities within hydrogels, thereby simulating narrow surgical margins and evaluating the responses of residual cells after resection to different treatments[181]. This further indicates that hydrogel-based drug models are no longer confined to drug screening alone, but are also being extended to clinical evaluation of postoperative recurrence risk and margin-directed therapeutic strategies.

CONSTRUCTION OF HYDROGEL-BASED INTEGRATED THERANOSTIC PLATFORMS

Theranostic integration is a key concept in modern precision medicine and is as important as cancer therapy itself. Its essence does not lie in simply co-loading diagnostic probes and therapeutic drugs into a single material system, but in integrating tumor recognition, drug delivery, and efficacy monitoring into one system through visual localization, microenvironment responsiveness, and local controlled release[182-183]. Hydrogels can form sustained therapeutic depots at tumor sites and can further incorporate diagnostic modules, thereby providing a material basis for the construction of integrated theranostic platforms. Recent studies indicate that multifunctional hydrogels are evolving from simple drug-delivery carriers into smart composite systems capable of combining diagnostic imaging with multiple therapeutic modalities [Figure 7].

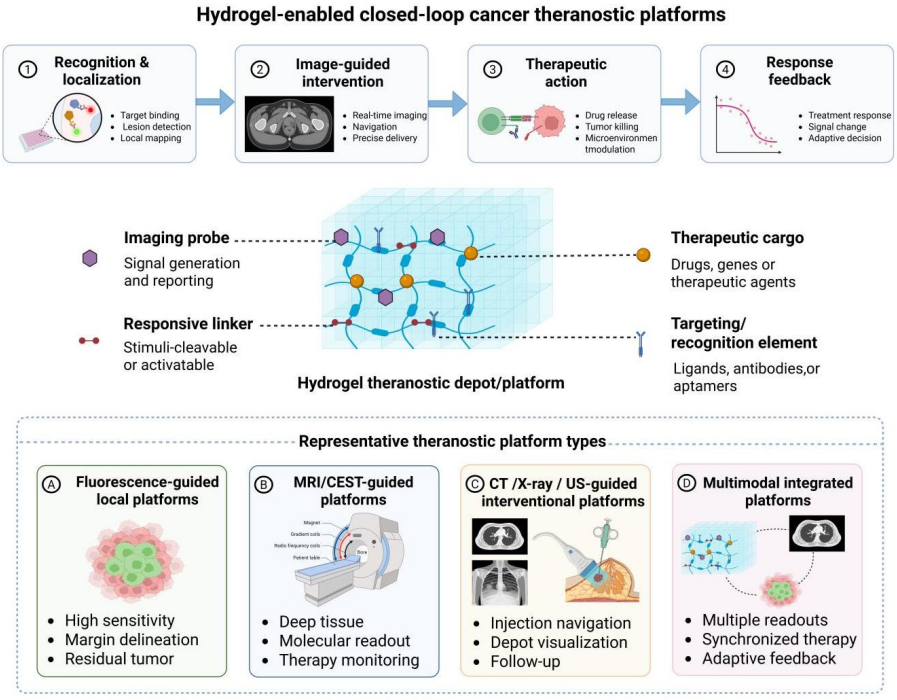


Figure 7. Schematic diagram of a hydrogel-mediated integrated tumor theranostic platform. The hydrogel simultaneously encapsulates imaging and therapeutic agents, enabling targeted or stimuli-responsive release through the design of the material matrix and gel network, thereby facilitating tumor recognition, treatment, and therapeutic feedback.(Figure was generated by BioRender, https://www.biorender.com/).

Fluorescence imaging-guided hydrogel theranostic platforms

Among hydrogel-based tumor theranostic platforms, fluorescence imaging-guided systems emerged earliest, are the most widely used, and are most readily coupled with therapeutic functions. Multiple clinical and translational studies have demonstrated that fluorescence imaging provides real-time spatial information for tumor identification and resection, facilitating tumor localization and lesion boundary visualization during surgery[184-186]. Unlike traditional paradigms in which efficacy is evaluated post-administration via changes in tumor volume, fluorescent hydrogels provide direct spatial information and dynamic feedback during treatment. They intuitively indicate whether the hydrogel has successfully reached the tumor region, remains locally retained, and whether the loaded drugs or functional nanocomponents have been released or activated[187-189]. Notably, when the

fluorescent component also possesses photothermal conversion, photodynamic effects, targeted recognition, or stimulus-responsive capabilities, the fluorescence signal transcends its role as a passive tracing tool. Instead, it becomes a functional interface linking tumor recognition, local delivery, treatment activation, and process monitoring[190-191]. At present, fluorescence imaging-guided hydrogel theranostic platforms are evolving from simple fluorescence tracing systems into integrated platforms combining imaging, targeting, controlled release, and multimodal therapy.

Fluorescent hydrogels represent the most extensively investigated format. By introducing fluorophores into hydrogels, local delivery can be visualized through fluorescence signals, thereby enabling real-time tracking of the therapeutic process[192-207][Table 1]. Many fluorescent materials themselves also possess photothermal conversion capability, allowing them to visualize tumors while simultaneously mediating therapy. For example, a fluorescent polydopamine nanoparticle composite hydrogel (FPNP-hydrogel) has been developed for fluorescence imaging-guided photothermal cancer therapy[208]. This FPNP-hydrogel was prepared by compositing fluorescent polydopamine nanoparticles (FPNPs) with PVA. The unique optical properties of FPNPs endowed the FPNP-hydrogel with excellent biocompatibility, strong fluorescence, and high photostability, enabling fluorescence imaging of tumor regions *in vivo*. At the same time, FPNPs also possess photothermal conversion capability and can generate marked temperature elevation under near-infrared laser irradiation, thereby killing tumor cells. These findings indicate that multifunctional hydrogels with excellent fluorescence performance and high photothermal conversion efficiency hold promise for the design of new cancer treatment strategies. Beyond incorporating fluorescent materials with photothermal properties, imaging, targeting, and therapeutic modules can also be integrated into a single gel system, enabling the platform to achieve precise molecular targeting and drug delivery while visualizing tumor localization. Ranjbar and colleagues[209] developed a mucin 1 (MUC1) aptamer-modified InP/ZnS quantum dot–nanohydrogel composite nanosystem co-loaded with paclitaxel and the lactate dehydrogenase inhibitor sodium oxamate. Through aptamer-mediated targeting of MCF-7 breast cancer cells, this system acquired fluorescence imaging capability from the quantum dots, enabling visualized recognition of tumor cells.

Meanwhile, the synergistic action of the loaded chemotherapeutic drug and glycolysis intervention enhanced tumor-cell inhibition and induced mitochondria-mediated apoptosis, supporting targeted recognition, imaging, and treatment of breast cancer and other solid tumors. Wang and colleagues further proposed a near-infrared-activated and ATP-responsive trifunctional upconversion nano-jelly system[210]. This gel used NaYF4 as the core matrix and was doped with Yb^{3+} and Er^{3+}, after which a silica shell loaded with methylene blue (MB) was constructed around it. A mesoporous silica layer was then introduced as a drug reservoir for DOX loading, and an anti-ATP aptamer sequence was assembled at the outermost layer to confer ATP responsiveness. Under near-infrared excitation, the gel core generated green emission at 540 nm for tumor imaging, while its red emission at 660 nm activated MB to produce singlet oxygen and induce a PDT effect. Meanwhile, the relatively high ATP level in tumor cells specifically binds to the outer aptamer, triggering disassembly of the DNA hydrogel network and thereby promoting DOX release, ultimately achieving synergistic integration of imaging, PDT, and chemotherapy. This also indicates that hydrogel theranostic platforms are advancing toward intelligent systems that are tumor-microenvironment responsive and exhibit multimodal therapeutic synergy.

Table 1. Summary of fluorescence-guided hydrogel theranostic platforms reported in the past three years.

Representative platform	Fluorescent component	Therapeutic component	Theranostic integration strategy	Application setting	Ref.
Injectable hyaluronic acid/carboxymethyl chitosan XCSgel platform	AF647	IL-12 and other cytokine-based local immunotherapy components	AF647-labeled immune mediators enable *in vitro* and *in vivo* fluorescence tracking to quantify intratumoral cytokine delivery, diffusion, and retention; XCSgel acts as a local drug depot that prolongs exposure to IL-12 and other immunomodulators and enhances antitumor immunotherapeutic efficacy.	Breast cancer	Mantooth S.M. *et al.*[192]
Injectable multifunctional	Coumarin	Doxorubicin (DOX)	The coumarin motif confers gel visualization capability	Solid tumor	Vu T.T. *et al.*[193]

Representative platform	Fluorescent component	Therapeutic component	Theranostic integration strategy	Application setting	Ref.
poly(N-acryloyl glycinamide)/alginate-derivative hydrogel platform			and serves as an NIR-responsive cleavage site; after NIR irradiation, gel decrosslinking rapidly releases DOX, thereby coupling imaging surveillance with on-demand chemotherapeutic delivery.		
MMP-responsive poly(glutamic acid)-based polypeptide hydrogel local drug-depot platform	Cy5/Cy3-labeled IgG	Oxaliplatin (OXA) + anti-PD-L1 antibody	Cy5/Cy3-labeled antibody/protein therapeutics enable visualization of release and intratumoral retention; the MMP-cleavable peptide-crosslinked network degrades in the tumor	Melanoma	Liang S. *et al.*[194]

Representative platform	Fluorescent component	Therapeutic component	Theranostic integration strategy	Application setting	Ref.
			MMP milieu to release OXA and anti-PD-L1, integrating release monitoring with chemotherapy-induced immunogenic cell death and immune-checkpoint blockade.		
Pluronic F127 *in situ* thermosensitive hydrogel platform	Rhodamine B (Rho B)	Atorvastatin (ATO) + cyclophosphamide (CTX)	Rho B serves as a small-molecule tracer to validate local tumor retention and sustained release from the F127 thermosensitive gel; the gel co-delivers ATO to downregulate PD-L1 and CTX to induce immunogenic	Colon cancer	Liu Z. *et al.*[195]

Representative platform	Fluorescent component	Therapeutic component	Theranostic integration strategy	Application setting	Ref.
			chemotherapy, forming a locally visualized chemo-immunotherapeutic regimen.		
Four-arm crosslinked injectable platform	PEG-chitosan hydrogel	PS2/porphine-derivative fluorescence	PS2 photosensitizer-mediated PDT	PS2 simultaneously serves as a fluorescent tracer/photosensitive component and participates in chitosan hydrogel construction; *in vivo* fluorescence imaging confirms intratumoral distribution and retention, whereas photoirradiation induces PS2-mediated ROS generation for PDT and antitumor immune	Colon cancer and melanoma	Gierlich P. *et al.*[196]

Representative platform	Fluorescent component	Therapeutic component	Theranostic integration strategy	Application setting	Ref.
			activation.		
Sodium alginate-calcium-genipin *in situ* reactive hydrogel platform	Genipin-tumor protein reaction products	*In situ*-generated photothermal agent/808 nm photothermal therapy	After intratumoral injection of the ACG hydrogel, genipin reacts with tumor proteins to form products with both fluorescent and photothermal properties; fluorescence imaging defines the optimal reaction/therapeutic window before NIR photothermal ablation.	Breast cancer	Wang Y. *et al.*[197]
AIE luminogen-modified MXene nanosheet/stimuli-responsive hydrogel platform	PEG-MeoTTPy AIE luminogen	MXene-mediated mild photothermal therapy + AIE photodynamic therapy/pyroptosis induction	AIEgen-coated MXene nanosheets are embedded in an Agar/PSBMA stimuli-responsive hydrogel; PEG-MeoTTPy provides NIR	Choroidal melanoma	Xu Y. *et al.*[198]

Representative platform	Fluorescent component	Therapeutic component	Theranostic integration strategy	Application setting	Ref.
			fluorescence and PDT capability, while MXene affords photothermal effects. NIR fluorescence/photothermal dual-modal imaging guides hydrogel-responsive release and synergistic mPTT/PDT.		
Nd/Mn co-doped whitlockite-sodium alginate composite hydrogel platform	Thermosensitive fluorescence of Nd/Mn co-doped whitlockite nanoparticles	Photothermal therapy + osteogenic/bone-repair material components	After incorporation of Nd/Mn co-doped whitlockite nanoparticles into sodium alginate hydrogel, temperature-dependent fluorescence intensity provides real-time thermal feedback; under irradiation, controllable	Osteosarcoma	Heng C. *et al.*[199]

Representative platform	Fluorescent component	Therapeutic component	Theranostic integration strategy	Application setting	Ref.
			photothermal ablation is achieved, while the whitlockite/sodium alginate matrix supports bone tissue repair.		
In situ injectable PEG-albumin hydrogel platform	ICG/Ce6	PTX chemotherapy + Ce6 PDT + ICG PTT + PFC oxygen supply	The PEG-albumin hydrogel encapsulates PTX-albumin nanoparticles and ICG/Ce6/PFC nanoemulsions; ICG/Ce6 provides fluorescent/photoresponsive therapeutic signals, whereas PFC alleviates hypoxia. Laser irradiation simultaneously triggers heat generation, singlet-	Breast cancer	Lee W.T. *et al.*[200]

Representative platform	Fluorescent component	Therapeutic component	Theranostic integration strategy	Application setting	Ref.
			oxygen production, and chemotherapy release, enabling imaging-assisted chemo/PDT/PTT combination therapy for hypoxic tumors.		
pH-responsive nanocomposite hydrogel platform based on dynamic boronate ester bonds	HA-ADH-RBITC fluorescent probe	Pt-TiO_2 sonosensitizer + imiquimod (IMQ) immunotherapeutic component	PLGA-BA and PVA form an acidic TME-responsive gel through dynamic boronate ester crosslinking; HA-ADH-RBITC enables tumor localization and fluorescence monitoring during treatment. Ultrasound-activated Pt-TiO_2 generates ROS, and IMQ activates T-cell	Breast cancer	Qian Z. *et al.*[201]

Representative platform	Fluorescent component	Therapeutic component	Theranostic integration strategy	Application setting	Ref.
			immunity, enabling imaging-guided sonodynamic-immunotherapy.		
MMP-responsive iridium(III)-based luminescent hydrogel platform	Lysosome-targeting iridium(III) complex emission	Iridium(III) complex-mediated PDT	The MMP-sensitive gel releases a lysosome-targeting iridium complex in cancer cells with high MMP activity, enabling cancer-cell-specific luminescence imaging; upon photoirradiation, the iridium complex induces lysosomal phototoxicity and suppresses cell migration, yielding an integrated imaging-targeted	MMP-overexpressing cancer cells	Yip A.M.H. *et al.*[202]

Representative platform	Fluorescent component	Therapeutic component	Theranostic integration strategy	Application setting	Ref.
			PDT platform. The PD-L1 aptamer confers residual-tumor targeting, while the lactate-responsive DNA network generates a detection signal and triggers therapeutic cargo release in the high-lactate postoperative microenvironment; ultrasound-activated Mito-US therapy eliminates residual tumor cells and establishes a postoperative detection-eradication feedback loop.		
PD-L1 aptamer-modified, lactate-responsive DNA hydrogel platform	Lactate-responsive DNA fluorescent reporter module	FX11-SPNT-mediated lactate metabolic intervention/mitochondria-targeted ultrasound therapy		Postoperative residual tumor detection and recurrence suppression	Liu Y. *et al.*[203]
Immunostimulatory *in*	Intrinsic	DOX DOX chemotherapy +	DOX@MPDA/M1NV is	Glioblastoma	Zhang R.

Representative platform	Fluorescent component	Therapeutic component	Theranostic integration strategy	Application setting	Ref.
situ fibrin gel platform	fluorescence/fluorescently labeled MPDA-M1NV nanovesicles	MPDA photothermal therapy + M1 macrophage-derived nanovesicle-mediated immune reprogramming	loaded into an *in situ* fibrin gel for postoperative local retention, and fluorescence imaging monitors gel/nanodrug distribution within the resection cavity; NIR irradiation triggers MPDA-mediated photothermal effects synergistic with DOX chemotherapy, while M1NV remodels tumor-associated macrophages to enhance postoperative photo-chemo-immunotherapy.		*et al.*[204]
Postoperative	CEA-responsive	Polydopamine-based	The implantable hydrogel	Residual	Geng S. *et al.*[205]

Representative platform	Fluorescent component	Therapeutic component	Theranostic integration strategy	Application setting	Ref.
implantable hydrogel platform	eMB/F sensor molecular beacon/eMB fluorescent nanoprobe	photothermal nanoprobe	integrates molecular beacon nanoprobes with fibroblasts and a gel scaffold, enabling ultrasensitive optical detection of residual microtumors through CEA-triggered signaling and Exo I cycle amplification; after visual localization, polydopamine nanoprobes mediate photothermal ablation to prevent postoperative recurrence and metastasis.	triple-negative breast cancer	
P407 thermosensitive hydrogel loaded with engineered	NIR fluorescence-labeled FOLactis	Engineered Lactococcus lactis secreting Flt3L-OX40L fusion protein	NIR fluorescence imaging verifies sustained release and local retention of	Peritoneal metastatic tumor	Chen A. *et al.*[206]

Representative platform	Fluorescent component	Therapeutic component	Theranostic integration strategy	Application setting	Ref.
Lactococcus lactis FOLactis			FOLactis from the P407 gel; after peritumoral injection, the thermosensitive gel forms an "artificial lymph island" that continuously releases engineered bacteria and activates dendritic cells and effector memory T cells, thereby enhancing bacterial immunotherapy.		
P407 thermosensitive hydrogel loaded with recombinant Mycobacterium smegmatis expressing IL-15	DiR NIR fluorescence-labeled Ms-IL15 (IVIS)	Recombinant Mycobacterium smegmatis expressing exogenous IL-15	DiR-labeled Ms-IL15 enables *in vivo* NIR imaging of engineered-bacterium release and retention within the P407 gel; intraperitoneal P407	Peritoneal metastatic tumor	Wang Q. *et al.*[207]

Representative platform	Fluorescent component	Therapeutic component	Theranostic integration strategy	Application setting	Ref.
			injection forms a local sustained-release depot that continuously releases IL-15-expressing engineered bacteria to promote DC maturation and memory T-cell differentiation while reducing M2 macrophage polarization.		

AF647: Alexa Fluor 647; IL-12: interleukin-12; XCSgel: cross-linked chitosan gel; Cy5: cyanine 5; Cy3: cyanine 3; IgG: immunoglobulin G; PD-L1: programmed death-ligand 1; F127: Pluronic F127/poloxamer 407; PEG: polyethylene glycol; PS2: photosensitizer 2; PDT: photodynamic therapy; ACG: sodium alginate-calcium-genipin; AIE: aggregation-induced emission; MXene: two-dimensional transition-metal carbide, nitride, or carbonitride; PEG-MeoTTPy: polyethylene glycol-modified MeoTTPy aggregation-induced-emission luminogen; article-specific compound code; PSBMA: poly(sulfobetaine methacrylate); mPTT: mild photothermal therapy; ICG: indocyanine green; Ce6: chlorin e6; PFC: perfluorocarbon; HA-ADH-RBITC: hyaluronic acid-adipic acid dihydrazide-rhodamine B isothiocyanate copolymer; ADH: adipic acid dihydrazide; RBITC: rhodamine B isothiocyanate; Pt: platinum; TiO2: titanium dioxide; Pt-TiO2: platinum-modified titanium dioxide; PLGA-BA: boronic acid-modified poly(L-glutamic acid); PVA: polyvinyl alcohol; FX11: lactate dehydrogenase A inhibitor FX11; SPNT: mitochondria-targeted semiconducting polymer nanoparticle/nanotransducer; article-specific platform code; FX11-SPNT: FX11-loaded mitochondria-targeted semiconducting polymer nanoparticle/nanotransducer; Mito-US:

mitochondria-targeted ultrasound therapy; MPDA: mesoporous polydopamine; M1NV: M1 macrophage-derived nanovesicle; CEA: carcinoembryonic antigen; eMB: exonuclease I-assisted molecular beacon; eMB/F: exonuclease I-assisted molecular beacon/fibroblast hydrogel sensor; Exo I: exonuclease I; P407: poloxamer 407; Flt3L: FMS-like tyrosine kinase 3 ligand; OX40L: OX40 ligand; Flt3L-OX40L: FMS-like tyrosine kinase 3 ligand-OX40 ligand fusion protein; FOLactis: Flt3L-OX40L-expressing Lactococcus lactis; DC: dendritic cell; DiR: 1,1'-dioctadecyl-3,3,3',3'-tetramethylindotricarbocyanine iodide; IL-15: interleukin-15; Ms-IL15: interleukin-15-expressing Mycobacterium smegmatis; IVIS: *in vivo* imaging system.

Radiological imaging-guided hydrogel theranostic platforms

Compared with fluorescent hydrogels, which primarily focus on optical tracing at the cellular or superficial tissue levels, image-guided hydrogels are more closely aligned with actual clinical treatment pathways and offer irreplaceable advantages in deep-tumor localization, interventional therapy, and three-dimensional anatomical assessment[211,212]. Their frontier value lies in the possibility not only of integrating diagnosis and treatment within a single system, but also of rendering the therapeutic process itself more controllable by linking *in vivo* hydrogel retention, release behavior, and efficacy changes to clinical imaging readouts. This offers a more translational technical strategy for precise local treatment of deep tumors and the construction of integrated theranostic platforms[213-225] [Table 2]

Table 2. Summary of image-guided hydrogel theranostic platforms reported in the past three years.

Theranostic content	Imaging/contrast component	Imaging modality	Treatment/intervention	Tumor model/type	Ref.

Theranostic content	Imaging/contrast component	Imaging modality	Treatment/intervention	Tumor model/type	Ref.
Silk fibroin hydrogel incorporating meglumine diatrizoate is X-ray visible and injectable *in situ*; local hydrogel-mediated release enhances osteosarcoma lesion control, enabling image-assisted focal therapy.	Meglumine diatrizoate (MD)	X-ray	Focal therapy/drug release	Osteosarcoma	Peng Z. *et al.*[213]
QCS/GA complex coacervates loaded with iohexol and DOX show shear-thinning behavior and X-ray opacity; they embolize VX2 tumor-feeding arteries and locally release DOX as a TACE-like platform.	Iohexol (the "I" in QCS/GA/I/DOX)	X-ray	TACE	Liver tumor	Liu M. *et al.*[214]
Drug molecules self-assemble into fibrous	Tantalum nanoparticles	X-ray	TACE + RT-enhanced immunity	Liver tumor	Peng Y. *et al.*[215]

Theranostic content	Imaging/contrast component	Imaging modality	Treatment/intervention	Tumor model/type	Ref.
hydrogels for X-ray-guided TACE; the platform combines embolization, sustained chemotherapeutic release, and radiotherapy-potentiated immunity for locoregional HCC treatment.	(Ta NPs)				
A radiopaque, radiation-responsive imiquimod-loaded hydrogel allows CT monitoring of delivery; combined with FLASH radiotherapy, it enhances local irradiation and immune activation in B16-F10 melanoma.	Gold nanoparticles (AuNPs)	CT/X-ray	FLASH RT + immunotherapy	Melanoma	Dong YC. *et al.*[216]
Iodinated poloxamer thermosensitive hydrogel	Iodixanol	X-ray/CT/CBCT	Local anticancer drug delivery	Solid tumor	Delgado JF. *et al.*[217]

Theranostic content	Imaging/contrast component	Imaging modality	Treatment/intervention	Tumor model/type	Ref.
gels at body temperature and can carry anticancer drugs; X-ray, CT, or CBCT visualizes the needle tract and gel distribution for image-guided local antitumor delivery.					
A CT-visible PLGA-PEG-PLGA thermosensitive immunoadjuvant gel is administered intratumorally and combined with cryoablation; sustained imiquimod release augments the abscopal effect.	Iopamidol	CT	Cryoablation + adjuvant/ICB	Solid tumor	Som A. *et al.*[218]
Magnetosomes incorporated into silk fibroin hydrogel form a magnetic hydrogel	Bacterial magnetosomes (Fe_3O_4	MRI	Magnetothermal therapy	Breast cancer	Huang G. *et al.*[219]

Theranostic content	Imaging/contrast component	Imaging modality	Treatment/intervention	Tumor model/type	Ref.
combining MRI localization with magnetothermal heating; it improves magnetothermal-agent retention and the controllability of image-guided tumor therapy.	magnetite nanocrystals/iron oxide magnetic core)				
A thermosensitive hydrogel delivers MRI-visible theranostic nanoprobes, combining chemotherapy and PTT to overcome MDR HCC; local gelation prolongs retention, and MRI monitors delivery and response.	Manganese oxide/manganese component in Au-MnO nanoparticles	MRI	Chemotherapy + PTT	Liver tumor	Huang S. *et al.*[220]
Fe_3O_4@Au core-shell nanocomposites are encapsulated in alginate	Fe_3O_4 magnetic core in Fe_3O_4@Au	MRI	DOX chemotherapy + PTT/magnetic targeting	Colorectal cancer	Khani T. *et al.*[221]

Theranostic content	Imaging/contrast component	Imaging modality	Treatment/intervention	Tumor model/type	Ref.
hydrogel and loaded with DOX; Fe_3O_4 enables MRI and magnetic targeting, whereas Au mediates photothermal conversion, enabling MRI-guided chemo-photothermal therapy. The Gd complex endows the hydrogel/scaffold with MRI capability for monitoring location and degradation, while MoS_2 provides photothermal effects; antibacterial and bone-repair functions support postoperative recurrence prevention and defect reconstruction in	core-shell nanocomposites Gadolinium-tetracarboxyphenylporphyrin complex (Gd-TCPP/Gd-complex)	MRI	PTT + antibacterial activity + bone reconstruction	Osteosarcoma	Huang Y. *et al.*[222]

Theranostic content	Imaging/contrast component	Imaging modality	Treatment/intervention	Tumor model/type	Ref.
osteosarcoma.					
CEST-detectable gemcitabine liposomes and methotrexate are incorporated into alginate hydrogel; CEST/APT signals track drug distribution and early response, supporting local chemotherapy for glioblastoma.	Exchangeable amine protons of gemcitabine (GEM) and methotrexate (MTX) (CEST 2.0-2.4 ppm)	CEST MRI	Local chemotherapy/monitoring	Glioblastoma	Park SW. *et al.*[223]
Fe_3O_4/gelatin magnetic colloidal hydrogel can be injected into HCC lesions under ultrasound guidance, followed by alternating magnetic field-triggered magnetothermal ablation; this reduces leakage and	Fe3O4-gelatin nanoparticle-based magnetic colloidal hydrogel matrix (MCH/MCH4)	Ultrasound guidance	Magnetothermal ablation	Liver tumor	Wu WS. *et al.*[224]

Theranostic content	Imaging/contrast component	Imaging modality	Treatment/intervention	Tumor model/type	Ref.
improves localized thermal killing. F127 hydrogel integrates ultrasound markers and the STING agonist MSA-2, enabling US-localized injection; combined with RFA for liver tumor ablation, it enhances local therapy and antitumor immunity.	Pluronic F127 hydrogel microbubbles (F127-MB)	Ultrasound	RFA + STING modulation	Liver tumor and colorectal cancer	Shen Y. *et al.*[225]

QCS: quaternized chitosan; GA: gum arabic; RT: radiotherapy; FLASH RT: ultra-high dose-rate radiotherapy; CBCT: cone-beam computed tomography; PLGA-PEG-PLGA: poly(lactic-co-glycolic acid)-polyethylene glycol-poly(lactic-co-glycolic acid); ICB: immune checkpoint blockade; PTT: photothermal therapy; MDR: multidrug resistance; APT: amide proton transfer; STING: stimulator of interferon genes; MSA-2: 4-(5,6-dimethoxybenzo[b]thiophen-2-yl)-4-oxobutanoic acid; RFA: radiofrequency ablation.

Paramagnetic ions enhance T1-weighted magnetic resonance imaging (MRI). Embedding such ions into hydrogels, therefore, enables real-time MRI monitoring and may also augment microwave ablation (MWA) by allowing polar water molecules within the gel to oscillate and generate frictional heat under a microwave field. On this basis, a minimalist manganese alginate (ALG-Mn) hydrogel was developed for MRI-guided synergistic antitumor therapy combining MWA and chemodynamic therapy[226]. In this system, Mn^{2+} not only crosslinks alginate to form an injectable hydrogel but also confers T1-weighted MRI visibility through its paramagnetism. At the same time, the abundance of Mn^{2+} and water molecules within the hydrogel enhances the local thermal effect under microwave irradiation, thereby improving the clearance efficiency of MWA against the primary tumor. After treatment, the ALG-Mn hydrogel continuously releases Mn^{2+}, which catalyzes intracellular ROS generation in the tumor microenvironment and further eradicates residual tumor cells that may survive MWA. Another breakthrough class of materials is magnetic nanoparticles (MNPs), which have increasingly become a research hotspot for reshaping cancer diagnosis and therapy. These materials enable real-time MRI monitoring and targeted tumor ablation via magnetic hyperthermia therapy (MHT), thereby reducing damage to surrounding healthy tissues[227]. Huang and colleagues constructed a magnetosome-incorporated silk fibroin magnetic hydrogel (MSMH)[219]. In this study, Fe_3O_4 magnetosomes were integrated with glycidyl methacrylate-modified silk fibroin, forming an *in situ* gel at the tumor site after intratumoral injection and subsequent ultraviolet irradiation, thereby immobilizing the magnetosomes locally. This hydrogel generated negative contrast enhancement on T2-weighted MRI to visualize local material distribution at the tumor site; subsequently, under an alternating magnetic field, the retained magnetosomes converted magnetic energy into heat, rapidly raising the local tumor temperature above the ablation threshold and thereby inducing tumor-cell apoptosis and necrosis to achieve MRI-assisted precision magnetic hyperthermia.

In contrast to conventional T1-/T2-weighted MRI, chemical exchange saturation transfer magnetic resonance imaging (CEST-MRI) generates signals through the exchange between exchangeable protons in molecules and water protons. CEST can therefore reveal molecular changes that are difficult to visualize directly by T1/T2 MRI[228]. When the hydrogel itself contains proton groups detectable by CEST, these groups can not only participate in therapy or delivery but also serve as trackable MRI signal sources. In one study, gemcitabine, detectable by CEST, was encapsulated in liposomes, whereas methotrexate was incorporated into an alginate hydrogel to endow the system with both sustained drug release and brain-tissue-compatible mechanical properties. Different parts-per-million (ppm) signals were utilized to track drug-related proton changes and amide proton transfer (APT) signals, thereby supporting local glioblastoma therapy and efficacy monitoring[223]. *In vivo* results demonstrated that changes in the APT signal preceded differences in tumor volume, indicating that CEST-MRI can capture molecular tumor responses before morphological changes become evident. Further regional analysis showed that areas adjacent to the hydrogel exhibited stronger therapeutic responses than areas farther away. These findings suggest that hydrogel platforms guided by multifrequency CEST signals can be used to monitor drug release, evaluate early therapeutic efficacy, and observe regional tumor responses, thereby providing a new design concept for image-guided theranostic platforms for brain tumors.

Beyond MRI and CEST-MRI, which monitor hydrogel treatment from the perspectives of tissue structure and molecular exchange, radiopaque hydrogels further extend material visualization to X-ray interventional guidance and computed tomography (CT)-assisted imaging[229]. X-ray fluoroscopy offers more direct procedural guidance in interventional oncology, especially for real-time visualization during transarterial catheter delivery and embolization[230]. Accordingly, introducing hydrophilic X-ray contrast agents into injectable hydrogels can render the gels radiopaque during intravascular delivery, thereby integrating image guidance, local embolization, and

multimodal therapy within a single interventional platform(Figure 8). Lee and colleagues[231] developed an iopamidol-doped radiopaque hydrogel for an X-ray fluoroscopy-guided hepatocellular carcinoma (HCC) transarterial chemo/starvation/chemodynamic embolization therapy (TACSCE) platform. The gel consisted of an HD network crosslinked by Mn ions and simultaneously incorporated glucose oxidase (GOx), DOX, and iopamidol. Iopamidol endowed the hydrogel with X-ray visibility, whereas catechol–Mn^{4+} coordination between HD and MnO_2 enabled the sol-to-gel transition required for local vascular embolization. Therapeutically, DOX provided sustained local chemotherapy; GOx consumed glucose in tumor cells while producing hydrogen peroxide (H_2O_2); and MnO_2 further induced a cascade killing effect through glutathione (GSH) depletion, O_2 generation, and Mn_2^+-mediated Fenton-like production of hydroxyl radicals (·OH). This study demonstrates that radiopaque hydrogels can integrate image guidance, vascular embolization, local chemotherapy, and tumor-microenvironment-responsive cascade catalysis into a transarterial theranostic platform for HCC. As early as 2019, imaging molecules and therapeutic drugs were co-encapsulated in liposomes for tumor diagnosis and therapy[232]. Traditional liposomal systems, however, are limited by payload leakage, particle instability, and burst release, and the widespread use of hydrogels has provided a new solution. By constructing a hydrogel core inside liposomes and co-loading iodinated contrast agents and chemotherapeutic drugs, hydrogel platforms can simultaneously improve contrast-agent retention, controlled drug release, and passive tumor accumulation, thereby creating CT-visualizable theranostic nanoplatforms. Sang and colleagues[233] developed a radiopaque hydrogel-in-liposome (RHL) nanoplatform in which iopamidol (IPD) and DOX were co-encapsulated as a micro-CT (μCT) contrast agent and chemotherapeutic drug, respectively, within a liposome-PEG hydrogel composite structure. The particle size of approximately 160 nm favors passive accumulation in tumors through the enhanced permeability and retention (EPR) effect, whereas the PEG hydrogel core inside the liposome reduces early DOX burst release and IPD leakage, thereby improving particle stability and *in vivo* delivery efficiency. *In*

vivo experiments showed that RHLs enhanced μCT contrast in tumor regions of SCCVII tumor-bearing mice and exhibited superior antitumor efficacy compared with conventional radiopaque liposomes and free DOX.

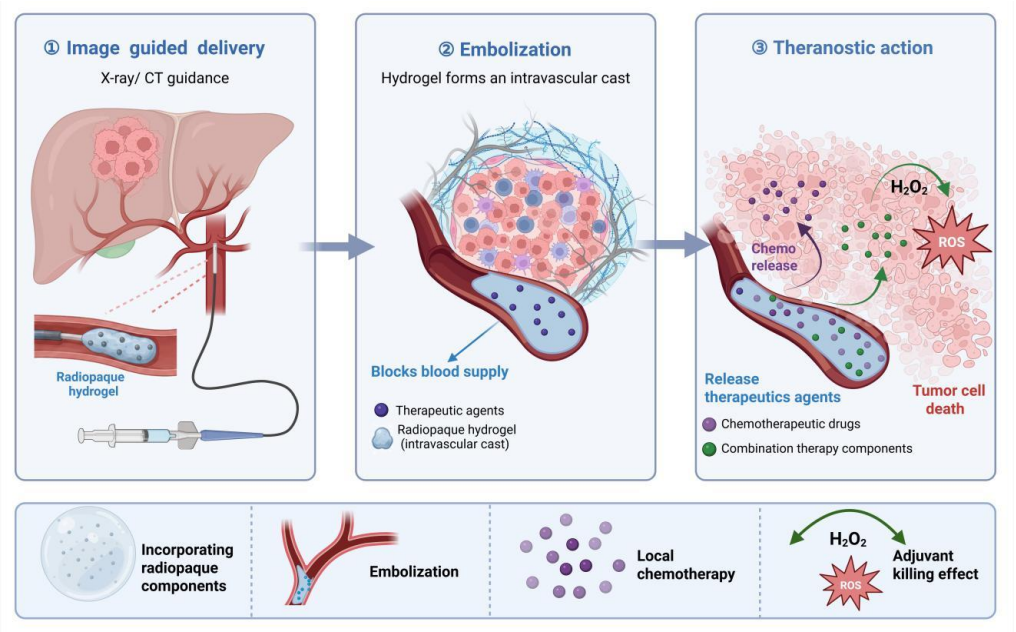


Figure 8. Schematic diagram of radiopaque hydrogel applied to tumor embolization. ① Injectable radiopaque hydrogel enables localization under imaging modalities such as X-ray; ② After injection, the hydrogel occludes the blood vessel; ③ Concurrently, therapeutic components are released for tumor eradication. (Figure was generated by BioRender, https://www.biorender.com/).

Hydrogel theranostic platforms integrating multimodal imaging and combination therapy

The direct significance of multimodal imaging integration lies in compensating for the limitations of any single imaging modality. Optical imaging offers high sensitivity, but its tissue penetration and clinical standardization remain limited[234]; MRI provides high soft-tissue resolution, but real-time interventional operation is less convenient than X-ray fluoroscopy[235]; CT and X-ray modalities are well suited for interventional navigation, but they provide limited information on molecular responses[236]; and

ultrasound (US) offers real-time, radiation-free, bedside applicability, but places higher demands on the acoustic properties of materials[237]. Accordingly, designing hydrogels that can be recognized simultaneously by two or more clinical imaging modalities helps to realize continuous monitoring from injection guidance and spatial distribution confirmation to post-treatment follow-up. Delgado and colleagues[238] reported in 2024 a thermosensitive poloxamer hydrogel that can be identified simultaneously by US, X-ray, and CT for localized hepatic therapy delivery. In this system, perfluorobutane-filled microbubbles enabled real-time visualization of the needle tip, needle tract, and gel-deposition region under B-mode US, whereas the incorporation of the iodinated contrast agent iodixanol rendered the hydrogel radiopaque under CT, cone-beam computed tomography (CBCT), and X-ray fluoroscopy, thereby enabling further confirmation of the spatial relationship between the gel and the target region through US/CT fusion and 3D reconstruction. Therapeutically, this poloxamer gel could load DOX and deliver it in a sustained manner. These findings suggest that dual-visible US/X-ray hydrogels may advance local drug delivery from blind injection toward image-guided theranostic platforms that are navigable, confirmable, and amenable to early follow-up. Building on multimodal imaging, the drug-loading capability and intelligent responsiveness of hydrogels also create opportunities to complement different therapies in time and space, ultimately yielding tumor theranostic systems that combine multimodal imaging, local controlled release, microenvironment responsiveness, and multiple treatment strategies. Hou and colleagues[239] constructed a folate-modified thermosensitive PCF-FAMXP composite hydrogel for targeted immunotherapy guided by dual-modality MRI/fluorescence imaging (FI). The core material, Fe_3O_4@Au, was coupled with Mn- or Zn-4-carboxyphenyl porphyrin (TCPP) and encapsulated within a polydopamine (PDA) membrane. In this system, Fe_3O_4/Mn-related components endowed the platform with T1-weighted MRI visibility, whereas the Mn-TCPP structure recovered fluorescence in tumor cells under the action of GSH and was used to track drug release and cellular uptake. Folate modification enabled tumor-cell recognition via folate receptors, and near-infrared irradiation induced thermoresponsive hydrogel dissolution,

promoting *in situ* release of FAMXP. After entering tumor cells, FAMXP released active components under acidic conditions and induced ICD through chemodynamic therapy (CDT), PDT, and PTT; when further combined with anti-PD-L1 immune checkpoint blockade, it enhanced CD^{4+}/CD^{8+} T-cell infiltration and antitumor immune responses.

CHALLENGES AND PERSPECTIVES

Current challenges

Hydrogel tumor theranostic platforms must first address the balance between local retention and long-term safety. Local retention is the basis for sustained drug release and imaging follow-up, but if the retention time does not overlap with the therapeutic window, safety risks may arise. Excessively rapid release can cause high local exposure and shorten the efficacy window, whereas overly slow degradation may induce foreign-body reactions, chronic inflammation, or accumulation of degradation products[240-242]. For composite hydrogels carrying metal ions, photothermal nanomaterials, imaging components, or immune adjuvants, long-term safety also involves the migration of nanocomponents and the intensity of local immune activation. Accordingly, evaluation of hydrogel platforms should not rely solely on short-term cytocompatibility, changes in tumor volume, or single release curves, but should also incorporate systematic validation of degradation-product toxicity, material residue, and late inflammatory responses.

Hydrogel networks exert dual effects on local retention and material exchange. On the one hand, their three-dimensional architecture can restrict the premature diffusion of drugs and functional nanocomponents, which is a key feature distinguishing hydrogels from free-drug administration; on the other hand, the same network may hinder the entry of low-abundance biomarkers, drug diffusion toward the tumor margin, immune-cell infiltration, and metabolite exchange[243-245]. In diagnostic settings, inappropriate design of mesh size and surface recognition sites may reduce the capture efficiency of

circulating tumor cells, extracellular vesicles, or nucleic acid biomarkers. In therapeutic settings, excessively strong local immobilization may lead to uneven drug distribution, causing overexposure in tissues adjacent to the gel while leaving distal tumor regions underdosed. For integrated theranostic systems, mass-transfer limitations may also create discrepancies between imaging signals and actual drug exposure, thereby compromising the accuracy of efficacy evaluation. Therefore, future material design should emphasize the quantitative relationships among network structure, diffusion pathways, and release kinetics, rather than simply pursuing higher crosslink densities or longer retention times.

A mismatch between stimulus-responsive mechanisms and the true tumor microenvironment remains a major limitation in current smart-hydrogel design. Many hydrogels rely on preset acidity, enzyme activity, redox state, or exogenous stimulation as release triggers; however, tumor tissue is not a single-variable system. Distinct cancer types, individual patients, and even different regions within the same tumor exhibit pronounced differences in vascular permeability, matrix density, hypoxia, and immune infiltration. Furthermore, these states continue to evolve following chemotherapy, photothermal therapy, or immunotherapy[246,247]. If the response threshold is set too low, the hydrogel may activate prematurely outside lesion sites; if set too high, the material may respond insufficiently within the tumor. More importantly, in integrated theranostic platforms, the response process simultaneously affects drug release, signal activation, and efficacy assessment, making it difficult for any single response mode to adapt to the continuously changing microenvironment during therapy. Thus, the essence of multi-responsive design lies not in simply stacking more trigger types, but in ensuring that material-response behavior matches the patient's tumor state and its dynamic evolution during treatment.

Hydrogel-guided integrated theranostic platforms may also exhibit performance interference among diagnostic, therapeutic, and feedback modules. The value of

hydrogel-based theranostics lies not in integrating all functional components into one material, but in functionally coupling localization, release, treatment, and monitoring. Enhancing imaging signals may require the introduction of inorganic or metallic components, yet such additions may increase residual risk or alter hydrogel mechanics. Increasing drug loading benefits local therapy but may compromise the stability of fluorescence, magnetic resonance, or photoacoustic signals. Similarly, incorporating photothermal, photodynamic, or immunomodulatory modules may intensify treatment but may also damage loaded proteins, nucleic acids, or living cells[248-250]. Therefore, multifunctional hydrogels should avoid the over-integration of functional modules. Instead, they should be designed minimally around specific clinical goals, employing strategies such as spatial partitioning or sequential release to reduce inter-module interference.

Finally, manufacturing consistency and clinical implementation remain practical barriers to the translation of hydrogel platforms. Complex composite hydrogels typically contain polymer matrices, crosslinking systems, nanocomponents, drugs, or bioactive payloads, and variation in any single parameter may influence performance[251]. Sterilization, lyophilization, reconstitution, transport, and long-term storage may further alter network structures, reduce the activity of proteins or cells, or trigger nanocomponent aggregation. Excessively expensive raw materials, preparation processes dependent on specialized equipment, and operational procedures that are difficult to standardize can all weaken feasibility across different medical settings. Moreover, animal models often fail to capture the anatomical complexity and treatment histories of patient tumors: a material that performs well in healthy subcutaneous tissue in animals does not necessarily remain stable in damaged surgical cavities, necrotic tumor margins, or post-radiotherapy tissues. Without models that replicate real delivery pathways, the evaluation of material performance is likely to remain confined to idealized settings.

Future perspectives

In response to these challenges, future hydrogel theranostic platforms will advance not merely by increasing material complexity, but by prioritizing individualization, clinical adaptability, and dynamic feedback. Unlike earlier validation strategies that relied primarily on standardized cell lines and animal models, next-generation hydrogel platforms must more accurately reflect patient-specific tumor heterogeneity, treatment-stage evolution, and actual delivery environments. A key foundation for this shift is the use of patient-derived organoids. Organoids partially preserve the tissue architecture, molecular characteristics, and drug-response patterns of primary tumors *in vitro*[252-253]. Consequently, they hold promise for pre-evaluating the compatibility between hydrogel theranostic platforms with diverse matrices and crosslinking strategies and specific patients, thereby reducing reliance on experience-driven material screening.

At the same time, advances in spatial omics provide higher-dimensional tissue information for the precise deployment of hydrogel platforms. By resolving intratumoral matrix density, immune-cell distribution, hypoxic regions, and boundaries at high risk of recurrence, spatial omics can help define the delivery range, response threshold, and release sequence of hydrogels, thereby shifting material design from a focus on single lesion characteristics to fine adaptation to tumor spatial heterogeneity. On this basis, artificial intelligence will become an important tool linking patient information with material parameters. By integrating material parameters, organoid drug-sensitivity data, spatial microenvironment information, and imaging/sensing data, artificial intelligence may predict how different design schemes will affect release behavior, imaging readouts, and therapeutic responses, thereby improving the predictability and personalization of hydrogel-platform development.

Finally, bioelectronic interfaces may endow hydrogel platforms with the capacity for continuous monitoring and feedback regulation. By combining conductive or injectable hydrogels with flexible electronic components, it may become possible to continuously

record temperature, pH, electrochemical, and inflammation-related signals after implantation or local administration. This assists in assessing material degradation, drug release, and therapeutic changes. Furthermore, biosafety must remain a core design constraint for next-generation hydrogel theranostic platforms. Developing hydrogel systems with clearly defined degradation pathways, low-toxicity degradation products, and efficient *in vivo* clearance is essential to avoid long-term residual risks caused by local retention and to promote the translation of hydrogels into clinically viable platforms that combine therapeutic efficacy with safety.

In summary, the future of hydrogel-driven integrated cancer theranostic platforms depends not only on the continued optimization of material composition, crosslinking architecture, and functional components, but also on achieving a deeper understanding of the complex interplay among hydrogel networks, the tumor microenvironment, and clinical delivery pathways. As technologies such as patient-derived organoids, spatial omics, artificial intelligence, and bioelectronic interfaces are progressively integrated into material design and efficacy evaluation, hydrogel platforms are expected to evolve into patient-information-driven, monitorable, and dynamically adjustable individualized theranostic systems, ultimately becoming core soft-material platforms that connect tumor recognition, local intervention, and therapeutic feedback.

DECLARATIONS

Authors' contribution

Conceptualization and design of the review: ZS.C; S.W; GS;

Literature search, data collection, and organization of the manuscript structure: X.M; M. C; LQ.C; Y.Z; L.C; YL.

Drafting of the manuscript: X.M; M.C; LQ.C;

Preparation and refinement of figures/tables: X.M.; M.C; Y.X; X.C;

Provided critical revisions and refined the manuscript for important intellectual content: S.W; ZS.C; G.S.

Availability of data and materials

Not applicable.

AI and AI-assisted tools statement

During the preparation of this manuscript, the AI tool ChatGPT (version 5.5) was used solely for language editing. The tool did not influence the study design, data collection, analysis, interpretation, or the scientific content of the work. All authors take full responsibility for the accuracy, integrity, and final content of the manuscript.

Financial support and sponsorship

This work was supported by the Natural Science Foundation of Hebei Province (Grant No. H2023209083) and the National Natural Science Foundation of China (Grant No. 82472636).

Conflicts of interest

All authors declared that there are no conflicts of interest.

Ethical approval and consent to participate

Not applicable.

Consent for publication

Not applicable.

Copyright

© The Author(s) 2026.

REFERENCE

[1] International Agency for Research on Cancer, Cancer Tomorrow - Estimated number of deaths for all cancers from 2022 to 2025 Available online: https://gco.iarc.fr/tomorrow/en/dataviz/isotype?years=2025&single_unit=500000&types=1 (accessed on July 30, 2024).

[2] Schwartzberg, L.; Kim, E. S.; Liu, D.; Schrag, D. Precision Oncology: Who, How, What, When, and When Not? *Am. Soc. Clin. Oncol. Educ. Book* 2017, 37, 160-9.[DOI: 10.1200/EDBK_174176]

[3] El-Deiry, W. S.; Goldberg, R. M.; Lenz, H. J.; et al. The current state of molecular testing in the treatment of patients with solid tumors, 2019. *CA Cancer J. Clin.* 2019, 69, 305-43.[DOI: 10.3322/caac.21560.]

[4] Kelkar, S. S.; Reineke, T. M. Theranostics: combining imaging and therapy. *Bioconjugate Chem.* 2011, 22, 1879-903.[DOI: 10.1021/bc200151q]

[5] Xie, Y.; Chen, Z. S. A caged drug enables precision delivery. *Science* 2025, 388, 1371-2.[DOI: 10.1126/science.ady9507]

[6] Gerlinger, M.; Rowan, A. J.; Horswell, S.; et al. Intratumor heterogeneity and branched evolution revealed by multiregion sequencing. *N. Engl. J. Med.* 2012, 366, 883-92.[DOI: 10.1056/NEJMoa1113205]

[7] Marusyk, A.; Janiszewska, M.; Polyak, K. Intratumor Heterogeneity: The Rosetta Stone of Therapy Resistance. *Cancer Cell* 2020, 37, 471-84.[DOI: 10.1016/j.ccell.2020.03.007]

[8] Bardelli, A.; Pantel, K. Liquid Biopsies, What We Do Not Know (Yet). *Cancer Cell* 2017, 31, 172-9.[DOI: 10.1016/j.ccell.2017.01.002]

[9] Collins, F. S.; Varmus, H. A new initiative on precision medicine. *N. Engl. J. Med.* 2015, 372, 793-5.[DOI: 10.1056/NEJMp1500523]

[10] Choi, K. Y.; Liu, G.; Lee, S.; Chen, X. Theranostic nanoplatforms for simultaneous cancer imaging and therapy: current approaches and future perspectives. *Nanoscale* 2012, 4, 330-42.[DOI: 10.1039/c1nr11277e]

[11] Rowe, S. P.; Pomper, M. G. Molecular imaging in oncology: Current impact and future directions. *CA Cancer J. Clin.* 2022, 72, 333-52.[DOI: 10.3322/caac.21713]

[12] O'Connor, J. P.; Aboagye, E. O.; Adams, J. E.; et al. Imaging biomarker roadmap for cancer studies. *Nat. Rev. Clin. Oncol.* 2017, 14, 169-86.[DOI: 10.1038/nrclinonc.2016.162]

[13] Mehta, P.; Sharma, M.; Devi, M. Hydrogels: An overview of its classifications, properties, and applications. *J. Mech. Behav. Biomed. Mater.* 2023, 147, 106145.[DOI: 10.1016/j.jmbbm.2023.106145]

[14] Li, J.; Mooney, D. J. Designing hydrogels for controlled drug delivery. *Nat. Rev. Mater.* 2016, 1, 16071.[DOI: 10.1038/natrevmats.2016.71]

[15] Sun, Z.; Song, C.; Wang, C.; Hu, Y.; Wu, J. Hydrogel-Based Controlled Drug Delivery for Cancer Treatment: A Review. *Mol. Pharm.* 2020, 17, 373-91.[DOI: 10.1021/acs.molpharmaceut.9b01020]

[16] Solanki, R.; Bhatia, D. Stimulus-Responsive Hydrogels for Targeted Cancer Therapy. *Gels* 2024, 10, 440.[DOI: 10.3390/gels10070440]

[17] Wichterle, O.; Lim, D. Hydrophilic gels for biological use. *Nature* 1960, 185, 117-8.[DOI: 10.1038/185117a0]

[18] Peppas, N. A.; Hilt, J. Z.; Khademhosseini, A.; Langer, R. Hydrogels in Biology and Medicine: From Molecular Principles to Bionanotechnology. *Adv. Mater.* 2006, 18, 1345-60.[DOI: 10.1002/adma.200501612]

[19] Hoffman, A. S. Hydrogels for biomedical applications. *Adv. Drug Deliv. Rev.* 2012, 64, 18-23.[DOI: 10.1016/j.addr.2012.09.010]

[20] Hoare, T. R.; Kohane, D. S. Hydrogels in drug delivery: Progress and challenges. *Polymer* 2008, 49, 1993-2007.[DOI: 10.1016/j.polymer.2008.01.027]

[21] Peppas, N. A.; Bures, P.; Leobandung, W.; Ichikawa, H. Hydrogels in pharmaceutical formulations. *Eur. J. Pharm. Biopharm.* 2000, 50, 27-46.[DOI: 10.1016/s0939-6411(00)00090-4]

[22] Tibbitt, M. W.; Anseth, K. S. Hydrogels as extracellular matrix mimics for 3D cell culture. *Biotechnol. Bioeng.* 2009, 103, 655-63.[DOI: 10.1002/bit.22361]

[23] Drury, J. L.; Mooney, D. J. Hydrogels for tissue engineering: Scaffold design variables and applications. *Biomaterials* 2003, 24, 4337-51.[DOI: 10.1016/S0142-9612(03)00340-5]

[24] Zhu, H.; Zheng, J.; Oh, X. Y.; et al. Nanoarchitecture-Integrated Hydrogel Systems toward Therapeutic Applications. *ACS Nano* 2023, 17, 7953-78.[DOI: 10.1021/acsnano.2c12448]

[25] Lu, P.; Ruan, D.; Huang, M.; et al. Harnessing the potential of hydrogels for advanced therapeutic applications: Current achievements and future directions. *Signal Transduct. Target. Ther.* 2024, 9, 166.[DOI: 10.1038/s41392-024-01852-x]

[26] Guo, L.; Fu, Z.; Li, H.; et al. Smart hydrogel: A new platform for cancer therapy. *Adv. Colloid Interface Sci.* 2025, 340, 103470.[DOI: 10.1016/j.cis.2025.103470]

[27] Lee, K. Y.; Mooney, D. J. Alginate: Properties and biomedical applications. *Prog. Polym. Sci.* 2012, 37, 106-26.[DOI: 10.1016/j.progpolymsci.2011.06.003]

[28] Augst, A. D.; Kong, H. J.; Mooney, D. J. Alginate hydrogels as biomaterials. *Macromol. Biosci.* 2006, 6, 623-33.[DOI: 10.1002/mabi.200600069]

[29] Rowley, J. A.; Madlambayan, G.; Mooney, D. J. Alginate hydrogels as synthetic extracellular matrix materials. *Biomaterials* 1999, 20, 45-53.[DOI: 10.1016/S0142-9612(98)00107-0]

[30] Dash, M.; Chiellini, F.; Ottenbrite, R. M.; Chiellini, E. Chitosan-A versatile semi-synthetic polymer in biomedical applications. *Prog. Polym. Sci.* 2011, 36, 981-1014.[DOI: 10.1016/j.progpolymsci.2011.02.001]

[31] Croisier, F.; Jérôme, C. Chitosan-based biomaterials for tissue engineering. *Eur. Polym. J.* 2013, 49, 780-92.[DOI: 10.1016/j.eurpolymj.2012.12.009]

[32] Sockett, K. A.; Jiang, N. C.; Ungolan, P.; Niu, J.; Grinstaff, M. W. Advancements in Hyaluronic Acid Synthetic Methodologies and Their Translational Relevance. *Chem. Rev.* 2026, 126, 3224-86.[DOI: 10.1021/acs.chemrev.5c00790]

[33] Burdick, J. A.; Prestwich, G. D. Hyaluronic Acid Hydrogels for Biomedical Applications. *Adv. Mater.* 2011, 23, H41-56.[DOI: 10.1002/adma.201003963]

[34] Highley, C. B.; Prestwich, G. D.; Burdick, J. A. Recent advances in hyaluronic acid hydrogels for biomedical applications. *Curr. Opin. Biotechnol.* 2016, 40, 35-40.[DOI: 10.1016/j.copbio.2016.02.008]

[35] Yue, K.; Trujillo-de Santiago, G.; Alvarez, M. M.; et al. Synthesis, properties, and biomedical applications of gelatin methacryloyl hydrogels. *Biomaterials* 2015, 73, 254-71.[DOI: 10.1016/j.biomaterials.2015.08.045]

[36] Caliari, S. R.; Burdick, J. A. A practical guide to hydrogels for cell culture. *Nat. Methods* 2016, 13, 405-14.[DOI: 10.1038/nmeth.3839]

[37] Gonzalez-Obeso, C.; Mogha, N. K.; Anand, S.; et al. Delivering on the promise of recombinant silk-inspired proteins for drug delivery. *Adv. Drug Deliv. Rev.* 2023, 192, 114622.[DOI: 10.1016/j.addr.2022.114622]

[38] Canal, T.; Peppas, N. A. Correlation between mesh size and equilibrium degree of swelling of polymeric networks. *J. Biomed. Mater. Res.* 1989, 23, 1183-93.[DOI: 10.1002/jbm.820231007]

[39] Zustiak, S. P.; Leach, J. B. Hydrolytically degradable poly(ethylene glycol) hydrogel scaffolds with tunable degradation and mechanical properties. *Biomacromolecules* 2010, 11, 1348-57.[DOI: 10.1021/bm100137q]

[40] Raeber, G. P.; Lutolf, M. P.; Hubbell, J. A. Molecularly engineered PEG hydrogels: a novel model system for proteolytically mediated cell migration. *Biophys. J.* 2005, 89, 1374-88.[DOI: 10.1529/biophysj.104.050682]

[41] Rehmann, M. S.; Skeens, K. M.; Kharkar, P. M.; et al. Tuning and predicting mesh size and protein release from step growth hydrogels. *Biomacromolecules* 2017, 18, 3131-42.[DOI: 10.1021/acs.biomac.7b00781]

[42] Lutolf, M. P.; Raeber, G. P.; Zisch, A. H.; Tirelli, N.; Hubbell, J. A. Cell-responsive synthetic hydrogels. Adv. Mater. 2003, 15, 888-92.[DOI: 10.1002/adma.200304621]

[43] Gill, B. J.; Gibbons, D. L.; Roudsari, L. C.; et al. A synthetic matrix with independently tunable biochemistry and mechanical properties to study epithelial

morphogenesis and EMT in a lung adenocarcinoma model. *Cancer Res.* 2012, 72, 6013-23.[DOI: 10.1158/0008-5472.CAN-12-0895]

[44] Li, J. K.; Wang, N.; Wu, X. S. Poly(vinyl alcohol) nanoparticles prepared by freezing-thawing process for protein/peptide drug delivery. *J. Control. Release* 1998, 56, 117-26.[DOI: 10.1016/S0168-3659(98)00089-3]

[45] Oh, N. G.; Hwang, S. Y.; Na, Y. H. Fabrication of a PVA-based hydrogel microneedle patch. *ACS Omega* 2022, 7, 25179-85.[DOI: 10.1021/acsomega.2c01993]

[46] Nguyen, H. X.; Bozorg, B. D.; Kim, Y.; et al. Poly(vinyl alcohol) microneedles: fabrication, characterization, and application for transdermal drug delivery of doxorubicin. *Eur. J. Pharm. Biopharm.* 2018, 129, 88-103.[DOI: 10.1016/j.ejpb.2018.05.017]

[47] Jain, M.; Pansuriya, R.; Thakur, R.; et al. PVA/guanidinium oleate transdermal patch as a pH-responsive drug delivery system for the localized and targeted delivery of anticancer drugs. *Mater. Adv.* 2024, 5, 1998-2011.[DOI: 10.1039/D3MA00346A]

[48] Tilghman, R. W.; Cowan, C. R.; Mih, J. D.; et al. Matrix rigidity regulates cancer cell growth and cellular phenotype. *PLOS One* 2010, 5, e12905.[DOI: 10.1371/journal.pone.0012905]

[49] Gao, Y.; Ren, F.; Ding, B.; et al. A thermo-sensitive PLGA-PEG-PLGA hydrogel for sustained release of docetaxel. *J. Drug Target.* 2011, 19, 516-27.[DOI: 10.3109/1061186X.2010.519031]

[50] Ma, H.; He, C.; Cheng, Y.; et al. PLK1shRNA and doxorubicin co-loaded thermosensitive PLGA-PEG-PLGA hydrogels for osteosarcoma treatment. *Biomaterials* 2014, 35, 8723-34.[DOI: 10.1016/j.biomaterials.2014.06.045]

[51] Zhang, S.; Holmes, T.; Lockshin, C.; Rich, A. Spontaneous assembly of a self-complementary oligopeptide to form a stable macroscopic membrane. *Proc. Natl. Acad. Sci. U. S. A.* 1993, 90, 3334-8.[DOI: 10.1073/pnas.90.8.3334]

[52] Hartgerink, J. D.; Beniash, E.; Stupp, S. I. Self-assembly and mineralization of peptide-amphiphile nanofibers. *Science* 2001, 294, 1684-8.[DOI: 10.1126/science.1063187]

[53] Um, S. H.; Lee, J. B.; Park, N.; Kwon, S. Y.; Umbach, C. C.; Luo, D. Enzyme-catalysed assembly of DNA hydrogel. *Nat. Mater.* 2006, 5, 797-801.[DOI: 10.1038/nmat1741]

[54] Xing, Y.; Cheng, E.; Yang, Y.; et al. Self-assembled DNA hydrogels with designable thermal and enzymatic responsiveness. *Adv. Mater.* 2011, 23, 1117-21.[DOI: 10.1002/adma.201003343]

[55] Rodell, C. B.; Kaminski, A. L.; Burdick, J. A. Rational design of network properties in guest-host assembled and shear-thinning hyaluronic acid hydrogels. *Biomacromolecules* 2013, 14, 4125-34.[DOI: 10.1021/bm401280z]

[56] Lin, C. C.; Anseth, K. S. PEG hydrogels for the controlled release of biomolecules in regenerative medicine. *Pharm. Res.* 2009, 26, 631-43.[DOI: 10.1007/s11095-008-9801-2]

[57] Censi, R.; Di Martino, P.; Vermonden, T.; Hennink, W. E. Hydrogels for protein delivery in tissue engineering. *J. Control. Release* 2012, 161, 680-92.[DOI: 10.1016/j.jconrel.2012.03.002]

[58] Appel, E. A.; del Barrio, J.; Loh, X. J.; et al. Self-assembled hydrogels utilizing polymer-nanoparticle interactions. *Nat. Commun.* 2015, 6, 6295.[DOI: 10.1038/ncomms7295]

[59] Jalalvandi, E.; Shavandi, A.; Whitelock, J.; et al. Shear thinning/self-healing hydrogel based on natural polymers with secondary photocrosslinking. *J. Mech Behav Biomed Mater.* 2019, 90, 191-201.[DOI: 10.1016/j.jmbbm.2018.10.009]

[60] Shi, Y.; Li, D.; He, C.; Chen, X. Design of an Injectable Polypeptide Hydrogel Depot Containing the Immune Checkpoint Blocker Anti-PD-L1 and Doxorubicin to Enhance Antitumor Combination Therapy. *Macromol. Biosci.* 2021, 21, e2100049.[DOI: 10.1002/mabi.202100049]

[61] Siboro, S. A. P.; Anugrah, D. S. B.; Ramesh, K.; et al. Tunable porosity of covalently crosslinked alginate-based hydrogels and its significance in drug release behavior. Carbohydr. *Polym.* 2021, 260, 117779.[DOI: 10.1016/j.carbpol.2021.117779]

[62] Fairbanks, B. D.; Schwartz, M. P.; Bowman, C. N.; Anseth, K. S. Photoinitiated polymerization of PEG-diacrylate with lithium phenyl-2,4,6-trimethylbenzoylphosphinate: polymerization rate and cytocompatibility. *Biomaterials* 2009, 30, 6702-7.[DOI: 10.1016/j.biomaterials.2009.08.055]

[63] Shin, G. R.; Hyun, H.; Lee, J.; et al. Injectable click-crosslinked hydrogel containing resveratrol to prevent breast cancer recurrence. *Mater Today Bio.* 2022, 16, 100386.DOI: 10.1016/j.mtbio.2022.100386]

[64] Cao, D.; Zhang, X.; Akabar, M. D.; et al. Liposomal doxorubicin loaded PLGA-PEG-PLGA based thermogel for sustained local drug delivery for the treatment of breast cancer. Artif. Cells Nanomed. *Biotechnol.* 2019, 47, 181-91.[DOI: 10.1080/21691401.2018.1548470]

[65] Nguyen, A. K.; Goering, P. L.; Reipa, V.; Narayan, R. J. Toxicity and photosensitizing assessment of gelatin methacryloyl-based hydrogels photoinitiated with lithium phenyl-2,4,6-trimethylbenzoylphosphinate in human primary renal proximal tubule epithelial cells. *Biointerphases* 2019, 14, 021007.[DOI: 10.1116/1.5095886]

[66] Nguyen, A. K.; Narayan, R. J. The photoinitiator lithium phenyl(2,4,6-trimethylbenzoyl)phosphinate with exposure to 405 nm light is cytotoxic to mammalian cells but not mutagenic in bacterial reverse mutation assays. *Polymers* 2020, 12, 1489.[DOI: 10.3390/polym12071489]

[67] Yesilyurt, V.; Ayoob, A. M.; Appel, E. A.; et al. Injectable self-healing glucose-responsive hydrogels with pH-regulated mechanical properties. *Adv. Mater.* 2016, 28, 86-91.[DOI: 10.1002/adma.201502902]

[68] Huang, Z.; Delparastan, P.; Burch, P.; et al. Injectable dynamic covalent hydrogels of boronic acid polymers cross-linked by bioactive plant-derived polyphenols. *Biomater.* Sci. 2018, 6, 2487-95.[DOI: 10.1039/C8BM00669D]

[69] Deng, C. C.; Brooks, W. L. A.; Abboud, K. A.; Sumerlin, B. S. Boronic Acid-Based Hydrogels Undergo Self-Healing at Neutral and Acidic pH. *ACS Macro Lett.* 2015, 4, 220-4.[DOI: 10.1021/acsmacrolett.5b00018]

[70] Lee, F.; Chung, J. E.; Kurisawa, M. An injectable enzymatically crosslinked hyaluronic acid hydrogel system with independent tuning of mechanical strength and gelation rate. *Soft Matter* 2008, 4, 880-7.[DOI: 10.1039/b719557e]

[71] Kurisawa, M.; Lee, F.; Wang, L. S.; Chung, J. E. Injectable enzymatically crosslinked hydrogel system with independent tuning of mechanical strength and gelation rate for drug delivery and tissue engineering. *J. Mater. Chem.* 2010, 20, 5371-5.[DOI: 10.1039/B926456F]

[72] Cheng, E.; Xing, Y.; Chen, P.; et al. A pH-triggered, fast-responding DNA hydrogel. *Angew. Chem., Int. Ed. Engl.* 2009, 48, 7660-3.[DOI: 10.1002/anie.200902538]

[73] Yang, H.; Liu, H.; Kang, H.; Tan, W. Engineering target-responsive hydrogels based on aptamer-target interactions. *J. Am. Chem. Soc.* 2008, 130, 6320-1.[DOI: 10.1021/ja801339w]

[74] Katopodi, T.; Petanidis, S.; Domvri, K.; et al. Hybrid nanogel drug delivery systems: transforming the tumor microenvironment through tumor tissue editing. *Cells* 2024, 13, 908.[DOI: 10.3390/cells13110908]

[75] Liu, Y.; Chen, L.; Shi, Q.; Zhao, Q.; Ma, H. Tumor microenvironment-responsive polypeptide nanogels for controlled antitumor drug delivery. *Front. Pharmacol.* 2021, 12, 748102.[DOI: 10.3389/fphar.2021.748102]

[76] Zhang, H.; Ba, S.; Lee, J. Y.; Xie, J.; Loh, T. P.; Li, T. Cancer biomarker-triggered disintegrable DNA nanogels for intelligent drug delivery. *Nano Lett.* 2020, 20, 8399-407.[DOI: 10.1021/acs.nanolett.0c03671]

[77] Xu, X.; Jiang, Y.; Lu, C. Self-assembled ATP-responsive DNA nanohydrogel for specifically activated fluorescence imaging and chemotherapy in cancer cells. *Anal. Chem.* 2022, 94, 10221-6.[DOI: 10.1021/acs.analchem.2c01760]

[78] Shang, J.; Yu, S.; Li, R.; He, Y.; Wang, Y.; Wang, F. Bioorthogonal disassembly of hierarchical DNAzyme nanogel for high-performance intracellular microRNA imaging. *Nano Lett.* 2023, 23, 1386-94.[DOI: 10.1021/acs.nanolett.2c04658]

[79] Su, M.; Zhu, Y.; Chen, J.; et al. Microfluidic synthesis of manganese-alginate nanogels with self-supplying H_2O_2 capability for synergistic chemo/chemodynamic therapy and boosting anticancer immunity. *Chem. Eng. J.* 2022, 435, 134926.[DOI: 10.1016/j.cej.2022.134926]

[80] Sanati, M.; Yavari, S. A. Liposome-integrated hydrogel hybrids: promising platforms for cancer therapy and tissue regeneration. *J. Control. Release* 2024, 368, 703-27.[DOI: 10.1016/j.jconrel.2024.03.008]

[81] Binaymotlagh, R.; Haghighi, F. H.; Chronopoulou, L.; Palocci, C. Liposome-hydrogel composites for controlled drug delivery applications. *Gels* 2024, 10, 284.[DOI: 10.3390/gels10040284]

[82] GuhaSarkar, S.; Pathak, K.; Sudhalkar, N.; et al. Synergistic locoregional chemoradiotherapy using a composite liposome-in-gel system as an injectable drug depot. *Int. J. Nanomedicine* 2016, 11, 6435-48.[DOI: 10.2147/IJN.S110525]

[83] Mao, Y.; Li, X.; Chen, G.; Wang, S. Thermosensitive hydrogel system with paclitaxel liposomes used in localized drug delivery system for in situ treatment of tumor: better antitumor efficacy and lower toxicity. *J. Pharm. Sci.* 2016, 105, 194-204.[DOI: 10.1002/jps.24693]

[84] Bouché, M.; Dong, Y. C.; Sheikh, S.; et al. Novel Treatment for Glioblastoma Delivered by a Radiation Responsive and Radiopaque Hydrogel. *ACS Biomater. Sci. Eng*. 2021, 7, 3209-20.[DOI: 10.1021/acsbiomaterials.1c00385]

[85] Huang, S.; Hong, X.; Zhao, M.; et al. Nanocomposite hydrogels for biomedical applications. *Bioeng. Transl. Med*. 2022, 7, e10315.[DOI: 10.1002/btm2.10315]

[86] Wang, C.; Zhao, N.; Huang, Y.; He, R.; Xu, S.; Yuan, W. Coordination of injectable self-healing hydrogel with Mn-Zn ferrite@mesoporous silica nanospheres for tumor MR imaging and efficient synergistic magnetothermal-chemo-chemodynamic therapy. *Chem. Eng. J.* 2020, 401, 126100.[DOI: 10.1016/j.cej.2020.126100]

[87] Yue, J.; Miao, P.; Li, L.; Yan, R.; Dong, W. F.; Mei, Q. Injectable carbon dots-based hydrogel for combined photothermal therapy and photodynamic therapy of cancer. *ACS Appl. Mater. Interfaces* 2022, 14, 49582-91.[DOI: 10.1021/acsami.2c15428]

[88] Battistelli, M. Liquid Biopsy: A Family of Possible Diagnostic Tools. *Diagnostics (Basel)* 2021, 11, 1391.[DOI: 10.3390/diagnostics11081391]

[89] Raza, A.; Khan, A. Q.; Inchakalody, V. P.; et al. Dynamic liquid biopsy components as predictive and prognostic biomarkers in colorectal cancer. *J. Exp. Clin. Cancer Res.* 2022, 41, 99.[DOI: 10.1186/s13046-022-02318-0]

[90] Kim, Y. J.; Min, J. Hydrogel-based technologies in liquid biopsy for the detection of circulating clinical markers: challenges and prospects. *Anal. Bioanal. Chem.* 2024, 416, 2065-78.[DOI: 10.1007/s00216-023-05025-7]

[91] Luchini, A.; Geho, D. H.; Bishop, B.; et al. Smart hydrogel particles: biomarker harvesting: one-step affinity purification, size exclusion, and protection against degradation. *Nano Lett.* 2008, 8, 350-61.[DOI: 10.1021/nl072174l]

[92] Tang, J.; Jia, X.; Li, Q.; et al. A DNA-based hydrogel for exosome separation and biomedical applications. *Proc. Natl. Acad. Sci. U. S. A.* 2023, 120, e2303822120.[DOI: 10.1073/pnas.2303822120]

[93] Sun, W.; You, X.; Zhao, X.; et al. Precise Capture and Dynamic Release of Circulating Liver Cancer Cells with Dual-Histidine-Based Cell Imprinted Hydrogels. *Adv. Mater.* 2024, 36, e2402379.[DOI: 10.1002/adma.202402379]

[94] Kim, Y. J.; Cho, Y. H.; Min, J.; Han, S. W. Circulating Tumor Marker Isolation with the Chemically Stable and Instantly Degradable (CSID) Hydrogel ImmunoSpheres. *Anal. Chem.* 2021, 93, 1100-9.[DOI: 10.1021/acs.analchem.0c04152]

[95] Kaniewska, K.; Kowalczyk, A.; Karbarz, M.; Nowicka, A. M. Changes in the volume phase transition temperature of hydrogels for detection of the DNA hybridization process. *Analyst* 2016, 141, 5815-21.[DOI: 10.1039/c6an00523c]

[96] Xu, Y.; Zhang, X.; Luan, C.; Wang, H.; Chen, B.; Zhao, Y. Hybrid hydrogel photonic barcodes for multiplex detection of tumor markers. *Biosens. Bioelectron.* 2017, 87, 264-70.[DOI: 10.1016/j.bios.2016.08.063.

[97] Sun, S.; Chen, J. Recent Advances in Hydrogel-Based Biosensors for Cancer Detection. *ACS Appl. Mater. Interfaces* 2024, 16, 46988-7002.[DOI: 10.1021/acsami.4c02317]

[98] Lu, H.; Samman, F.; Hasan, E.; Alsulaiman, D. Novabeads: Stimuli-Responsive Signal-Amplifying Hydrogel Microparticles for Enzymeless Fluorescence-Based Detection of microRNA Biomarkers. *Small* 2025, 21, e2503990.[DOI: 10.1002/smll.202503990]

[99] Ring, A.; Nguyen-Sträuli, B. D.; Wicki, A.; Aceto, N. Biology, vulnerabilities and clinical applications of circulating tumour cells. *Nat. Rev. Cancer* 2023, 23, 95-111.[DOI: 10.1038/s41568-022-00536-4.

[100] Capuozzo, M.; Ferrara, F.; Santorsola, M.; Zovi, A.; Ottaiano, A. Circulating Tumor Cells as Predictive and Prognostic Biomarkers in Solid Tumors. *Cells* 2023, 12, 2590.[DOI: 10.3390/cells12222590]

[101] Portella, L.; Bertolini, G.; Guardascione, G.; et al. CXCL12-loaded-hydrogel (CLG): A new device for metastatic circulating tumor cells (CTCs) capturing and characterization. *Heliyon* 2024, 10, e35524.[DOI: 10.1016/j.heliyon.2024.e35524]

[102] Chen, B.; Wang, G.; Huang, C.; et al. A light-induced hydrogel responsive platform to capture and selectively isolate single circulating tumor cells. *Nanoscale* 2022, 14, 3504-3512.[DOI: 10.1039/d1nr06876h]

[103] Dawson, S. J.; Tsui, D. W.; Murtaza, M.; et al. Analysis of circulating tumor DNA to monitor metastatic breast cancer. *N. Engl. J. Med.* 2013, 368, 1199-209.[DOI: 10.1056/NEJMoa1213261]

[104] Garcia-Murillas, I.; Schiavon, G.; Weigelt, B.; et al. Mutation tracking in circulating tumor DNA predicts relapse in early breast cancer. *Sci. Transl. Med.* 2015, 7, 302ra133.[DOI: 10.1126/scitranslmed.aab0021]

[105] Zhao, X.; Meng, X.; Zeng, X.; He, T.; Chen, J.; Chen, P. Homogeneous Extraction-Free Dual-ctDNA Detection via DNA Nanomaterial Fusion for Rapid Breast Cancer Diagnosis. *ACS Nano* 2025, 19, 42066-78.[DOI: 10.1021/acsnano.5c11295]

[106] Hou, J.; Wang, Y.; Yuan, W.; et al. Thermosensitive hydrogel-enhanced RPA-CRISPR/Cas12a biosensor for ultrasensitive detection of methylated loci in breast cancer ctDNA. *Anal. Chim. Acta* 2026, 1388, 345101.[DOI: 10.1016/j.aca.2026.345101]

[107] McAlexander, M. A.; Phillips, M. J.; Witwer, K. W. Comparison of Methods for miRNA Extraction from Plasma and Quantitative Recovery of RNA from Cerebrospinal Fluid. *Front. Genet.* 2013, 4, 83.[DOI: 10.3389/fgene.2013.00083]

[108] Sourvinou, I. S.; Markou, A.; Lianidou, E. S. Quantification of circulating miRNAs in plasma: effect of preanalytical and analytical parameters on their isolation and stability. *J. Mol. Diagn.* 2013, 15, 827-34.[DOI: 10.1016/j.jmoldx.2013.07.005]

[109] Jang, W.; Kim, Y. J.; Roh, H. K.; Song, E. L.; Bong, K. W. Hydrogel-Based In Situ DNA Extension Assay for Multiplexed and Rapid Detection of MicroRNA. *Anal. Chem.* 2025, 97, 7317-24.[DOI: 10.1021/acs.analchem.4c06995]

[110] Chen, D.; Wang, Y.; Wei, Y.; et al. Size-Coded Hydrogel Microbeads for Extraction-Free Serum Multi-miRNAs Quantifications with Machine-Learning-Aided Lung Cancer Subtypes Classification. *Nano Lett.* 2025, 25, 453-60.[DOI: 10.1021/acs.nanolett.4c05233]

[111] Lin, Y.; Xing, G.; Wu, Z.; et al. Microfluidic-Enabled Self-Directed Hydrogel Microspheres for Multiplexed MicroRNA Assays. *Anal. Chem.* 2025, 97, 1972-76.[DOI: 10.1021/acs.analchem.4c05349]

[112] Yao, C.; Wang, Q.; Lu, X.; Chen, X.; Li, Z. Hydrogel-Based Microdroplet Ensembles Encapsulating Multiplexed EXPAR Assays for Trichromic Digital Profiling of MicroRNAs and in-Depth Classification of Primary Urethral Cancers. *Nano Lett.* 2024, 24, 15861-9.[DOI: 10.1021/acs.nanolett.4c04898]

[113] Yu, W.; Hurley, J.; Roberts, D.; et al. Exosome-based liquid biopsies in cancer: opportunities and challenges. *Ann. Oncol.* 2021, 32, 466-77.[DOI: 10.1016/j.annonc.2021.01.074]

[114] Xu, X.; Zhang, M.; Zhang, X.; et al. Decoding Expression Dynamics of Protein and Transcriptome at the Single-Cell Level in Paired Picoliter Chambers. *Anal. Chem.* 2022, 94, 8164-73.[DOI: 10.1021/acs.analchem.1c05312]

[115] Miwa, H.; Dimatteo, R.; de Rutte, J.; Ghosh, R.; Di Carlo, D. Single-cell sorting based on secreted products for functionally defined cell therapies. *Microsyst. Nanoeng.* 2022, 8, 84.[DOI: 10.1038/s41378-022-00422-x]

[116] Yamagata, C.; Hamazaki, Y.; Nakazato, T.; et al. Oil-sealed RGD-modified alginate hydrogel microwell array for analysis of single-cell-derived extracellular vesicles and particles. *Microsyst. Nanoeng.* 2025, 11, 238.[DOI: 10.1038/s41378-025-01092-1]

[117] Lee, S. S.; Kim, H.; Sohn, D. K.; et al. Indocyanine green-loaded injectable alginate hydrogel as a marker for precision cancer surgery. *Quant. Imaging Med. Surg.* 2020, 10, 779-88.[DOI: 10.21037/qims.2020.02.24]

[118] Linders, D. G. J.; Bijlstra, O. D.; Walker, E.; et al. Ex vivo fluorescence-guided resection margin assessment in breast cancer surgery using a topically applied, cathepsin-activatable imaging agent. *Pharmacol. Res.* 2024, 209, 107464.[DOI: 10.1016/j.phrs.2024.107464]

[119] Yang, H. Y.; Jang, M. S.; Sun, X. S.; et al. CD44-mediated tumor homing of hyaluronic acid nanogels for hypoxia-activated photodynamic therapy against tumor. Colloids Surf. *B Biointerfaces* 2023, 228, 113395.[DOI: 10.1016/j.colsurfb.2023.113395]

[120] Song, P.; Ye, D.; Zuo, X.; et al. DNA Hydrogel with Aptamer-Toehold-Based Recognition, Cloaking, and Decloaking of Circulating Tumor Cells for Live Cell Analysis. *Nano Lett.* 2017, 17, 5193-8.[DOI: 10.1021/acs.nanolett.7b01006]

[121] Chen, T.; Su, L.; Lin, L.; et al. Mesoporous radiosensitized nanoprobe for enhanced NIR-II photoacoustic imaging-guided accurate radio-chemotherapy. *Nano Res.* 2022, 15, 4154-63.[DOI: 10.1007/s12274-021-3997-4]

[122] Vahrmeijer, A. L.; Hutteman, M.; van der Vorst, J. R.; et al. Image-guided cancer surgery using near-infrared fluorescence. Nat. Rev. *Clin. Oncol.* 2013, 10, 507-18.[DOI: 10.1038/nrclinonc.2013.123]

[123] Saxena, V.; Sadoqi, M.; Shao, J. Degradation kinetics of indocyanine green in aqueous solution. *J. Pharm. Sci.* 2003, 92, 2090-7.[DOI: 10.1002/jps.10470]

[124] Andreiuk, B.; Reisch, A.; Bernhardt, E.; Klymchenko, A. S. Fighting aggregation-caused quenching and leakage of dyes in fluorescent polymer nanoparticles: universal role of counterion. *Chem. Asian J.* 2019, 14, 836-46.[DOI: 10.1002/asia.201801592]

[125] Liu, C.; Ruan, C.; Shi, R.; Jiang, B.; Ji, S.; Shen, X. A near infrared-modulated thermosensitive hydrogel for stabilization of indocyanine green and combinatorial anticancer phototherapy. *Biomater. Sci.* 2019, 7, 1705-15.[DOI: 10.1039/C8BM01541D]

[126] Masaeli, E.; Srinivasan, S.; Rajabzadeh, A. R. Transforming cancer diagnosis and therapy through fluorescent hydrogels: a review. *Adv. Healthc. Mater.* 2026, 15, e202502577.[DOI: 10.1002/adhm.202502577]

[127] Park, J.; Ku, M.; Kim, E.; et al. CD44-specific supramolecular hydrogels for fluorescence molecular imaging of stem-like gastric cancer cells. *Integr. Biol. (Camb.)* 2013, 5, 669-72.[DOI: 10.1039/c3ib20203h]

[128] Yang, J.; Qu, J.; Teng, X.; et al. Tumor Microenvironment-Responsive Hydrogel for Direct Extracellular ATP Imaging-Guided Surgical Resection with Clear Boundaries. *Adv. Healthc. Mater.* 2023, 12, e2301084.[DOI: 10.1002/adhm.202301084]

[129] Walker, E.; Linders, D. G. J.; Abenojar, E.; et al. Formulation of a Thermosensitive Imaging Hydrogel for Topical Application and Rapid Visualization of Tumor Margins in the Surgical Cavity. *Cancers (Basel)* 2022, 14, 3459.[DOI: 10.3390/cancers14143459]

[130] Guo, P.; Qi, A.; Shang, W.; et al. Targeting tumour surface collage with hydrogel probe: a new strategy to enhance intraoperative imaging sensitivity and stability of bladder cancer. *Eur. J. Nucl. Med. Mol. Imaging* 2024, 51, 4165-76.[DOI: 10.1007/s00259-024-06848-x]

[131] Lee, S. S.; Choi, Y. Near-Infrared Dye-Loaded Thermosensitive Hydrogels as Novel Fluorescence Tissue Markers. *Gels* 2025, 11, 649.[DOI: 10.3390/gels11080649]

[132] Upputuri, P. K.; Pramanik, M. Photoacoustic imaging in the second near-infrared window: a review. *J. Biomed. Opt.* 2019, 24, 040901.[DOI: 10.1117/1.JBO.24.4.040901]

[133] Sun, X.; Li, Y.; Liu, X.; Cui, D.; Shi, Y.; Huang, G. Tumor-specific enhanced NIR-II photoacoustic imaging via photothermal and low-pH coactivated AuNR@PNIPAM-VAA nanogel. *J. Nanobiotechnology* 2024, 22, 326.[DOI: 10.1186/s12951-024-02617-y]

[134] Jo, J.; Folz, J.; Gonzalez, M. E.; et al. Personalized Oncology by In Vivo Chemical Imaging: Photoacoustic Mapping of Tumor Oxygen Predicts Radiotherapy Efficacy. *ACS Nano* 2023, 17, 4396-403.[DOI: 10.1021/acsnano.2c09502]

[135] Folz, J.; Jo, J.; Eido, A.; et al. Photoacoustic Chemical Imaging of Tumor Microenvironment pH for Prediction of Chemotherapeutic Efficacy in Breast Cancer. *Nano Lett.* 2025, 25, 14808-16.[DOI: 10.1021/acs.nanolett.5c02756]

[136] Tyler, B.; Fowers, K. D.; Li, K. W.; et al. A thermal gel depot for local delivery of paclitaxel to treat experimental brain tumors in rats. *J. Neurosurg.* 2010, 113, 210-7.[DOI: 10.3171/2009.11.JNS08162]

[137] Wang, C.; Wang, J.; Zhang, X.; et al. In situ formed reactive oxygen species-responsive scaffold with gemcitabine and checkpoint inhibitor for combination therapy. *Sci. Transl. Med.* 2018, 10, eaan3682.[DOI: 10.1126/scitranslmed.aan3682]

[138] Chen, Q.; Wang, C.; Zhang, X.; et al. In situ sprayed bioresponsive immunotherapeutic gel for post-surgical cancer treatment. *Nat. Nanotechnol.* 2019, 14, 89-97.[DOI: 10.1038/s41565-018-0319-4]

[139] Liu, Y.; Han, Y.; Lu, S.; et al. Injectable hydrogel platform with biodegradable Dawson-type polyoxometalate and R848 for combinational photothermal-immunotherapy of cancer. *Biomater. Sci.* 2022, 10, 1257-66.[DOI: 10.1039/D1BM01835C]

[140] Zhao, J.; Li, J.; Zhu, C.; et al. Design of phase-changeable and injectable alginate hydrogel for imaging-guided tumor hyperthermia and chemotherapy. *ACS Appl. Mater. Interfaces* 2018, 10, 3392-404.[DOI: 10.1021/acsami.7b17608]

[141] Shi, J.; Kantoff, P. W.; Wooster, R.; Farokhzad, O. C. Cancer nanomedicine: progress, challenges and opportunities. *Nat. Rev. Cancer* 2017, 17, 20-37.[DOI: 10.1038/nrc.2016.108]

[142] Guo, Y.; Chen, Y.; Wu, Y.; et al. Injectable pH-responsive polypeptide hydrogels for local delivery of doxorubicin. *Nanoscale Adv.* 2024, 6, 6420-32.[DOI: 10.1039/D4NA00719K]

[143] Shi, Y.; Zhu, H.; Xu, S.; et al. Injectable doxorubicin-loaded hyaluronic acid-based hydrogel for locoregional therapy and inhibiting metastasis of breast cancer. *Colloids Surf. B Biointerfaces* 2025, 247, 114433.[DOI: 10.1016/j.colsurfb.2024.114433]

[144] Zhang, Q.; Zhang, Y.; Chen, H.; et al. Injectable hydrogel with doxorubicin-loaded ZIF-8 nanoparticles for tumor postoperative treatments and wound repair. *Sci. Rep.* 2024, 14, 9983.[DOI: 10.1038/s41598-024-57664-0]

[145] Donnelly, R. F.; Singh, T. R. R.; Garland, M. J.; et al. Hydrogel-forming microneedle arrays for enhanced transdermal drug delivery. *Adv. Funct. Mater.* 2012, 22, 4879-90.[DOI: 10.1002/adfm.201200864]

[146] Zhu, L.; Qiao, G.; Gao, H.; Jiang, A.; Zhang, L.; Wang, X. Enhancing melanoma therapy with hydrogel microneedles. *Front. Oncol.* 2025, 15, 1590534.[DOI: 10.3389/fonc.2025.1590534]

[147] Wang, C.; Ye, Y.; Hochu, G. M.; Sadeghifar, H.; Gu, Z. Enhanced cancer immunotherapy by microneedle patch-assisted delivery of anti-PD1 antibody. *Nano Lett.* 2016, 16, 2334-40.[DOI: 10.1021/acs.nanolett.5b05030]

[148] Zhang, Z.; Zhang, Z.; Zeng, W.; Li, Y.; Zhu, C. A hyaluronic acid-based dual-functional hydrogel microneedle system for sequential melanoma ablation and skin regeneration. *Int. J. Biol. Macromol.* 2024, 283, 138039.[DOI: 10.1016/j.ijbiomac.2024.138039]

[149] Messing, E. M.; Tangen, C. M.; Lerner, S. P.; et al. Effect of intravesical instillation of gemcitabine vs saline immediately following resection of suspected low-grade non-muscle-invasive bladder cancer on tumor recurrence: SWOG S0337 randomized clinical trial. *JAMA* 2018, 319, 1880-8.[DOI: 10.1001/jama.2018.4657]

[150] Zheng, B.; Zhang, H.; Wang, J.; et al. A mucoadhesive-to-penetrating nanomotors-in-hydrogel system for urothelium-oriented intravesical drug delivery. *J. Nanobiotechnology* 2024, 22, 560.[DOI: 10.1186/s12951-024-02816-7]

[151] Sahin, U.; Derhovanessian, E.; Miller, M.; et al. Personalized RNA mutanome vaccines mobilize poly-specific therapeutic immunity against cancer. *Nature* 2017, 547, 222-6.[DOI: 10.1038/nature23003]

[152] Ott, P. A.; Hu, Z.; Keskin, D. B.; et al. An immunogenic personal neoantigen vaccine for patients with melanoma. *Nature* 2017, 547, 217-21.[DOI: 10.1038/nature22991]

[153] Gong, N.; Alameh, M. G.; El-Mayta, R.; Xue, L.; Weissman, D.; Mitchell, M. J. Enhancing in situ cancer vaccines using delivery technologies. *Nat. Rev. Drug Discov.* 2024, 23, 607-25.[DOI: 10.1038/s41573-024-00974-9]

[154] Sakuishi, K.; Apetoh, L.; Sullivan, J. M.; Blazar, B. R.; Kuchroo, V. K.; Anderson, A. C. Targeting Tim-3 and PD-1 pathways to reverse T cell exhaustion and restore anti-tumor immunity. *J. Exp. Med.* 2010, 207, 2187-94.[DOI: 10.1084/jem.20100643]

[155] Fan, S.; Han, H.; Yan, Z.; Lu, Y.; He, B.; Zhang, Q. Lipid-based nanoparticles for cancer immunotherapy. *Med. Rev.* (2021) 2023, 3, 230-69.[DOI: 10.1515/mr-2023-0020]

[156] Mikhail, A. S.; Morhard, R.; Mauda-Havakuk, M.; Kassin, M.; Arrichiello, A.; Wood, B. J. Hydrogel drug delivery systems for minimally invasive local immunotherapy of cancer. *Adv. Drug Deliv. Rev.* 2023, 202, 115083.[DOI: 10.1016/j.addr.2023.115083]

[157] Pechnikova, N. A.; Aggeli, A.; Latypova, A. A.; et al. Implantable Biomaterials for Cancer Immunotherapies. *Adv. Funct. Mater.* 2025, 35, 2416813.[DOI: 10.1002/adfm.202416813]

[158] Jia, W.; Wu, Y.; Xie, Y.; Yu, M.; Chen, Y. Advanced Polymeric Nanoparticles for Cancer Immunotherapy: Materials Engineering, Immunotherapeutic Mechanism and Clinical Translation. *Adv. Mater.* 2025, 37, e2413603.[DOI: 10.1002/adma.202413603]

[159] Qiu, W.; Zheng, Y.; Shen, F.; et al. Rapid hemostasis tumor in situ hydrogel vaccines for colorectal cancer chemo-immunotherapy. *ACS Appl. Mater. Interfaces* 2024, 16, 61679-91.[DOI: 10.1021/acsami.4c13489]

[160] Ji, P.; Sun, W.; Zhang, S.; et al. Modular hydrogel vaccine for programmable and coordinate elicitation of cancer immunotherapy. *Adv. Sci. (Weinh.)* 2023, 10, e2301789.[DOI: 10.1002/advs.202301789]

[161] Zhao, X.; Xuan, F.; Li, Z.; et al. A KIF20A-based thermosensitive hydrogel vaccine effectively potentiates immune checkpoint blockade therapy for hepatocellular carcinoma. *NPJ Vaccines* 2025, 10, 1.[DOI: 10.1038/s41541-024-01060-2]

[162] Wang, Z.; Qiu, S.; Sun, Y.; et al. An injectable oncolytic hydrogel platform for in situ dendritic cell vaccination to boost antitumor immunity. *Biomater. Sci.* 2025, 13, 3016-29.[DOI: 10.1039/D5BM00284B]

[163] Kenny, H. A.; Krausz, T.; Yamada, S. D.; Lengyel, E. Use of a novel 3D culture model to elucidate the role of mesothelial cells, fibroblasts and extracellular matrices on adhesion and invasion of ovarian cancer cells to the omentum. *Int. J. Cancer* 2007, 121, 1463-72.[DOI: 10.1002/ijc.22874]

[164] Fischbach, C.; Chen, R.; Matsumoto, T.; et al. Engineering tumors with 3D scaffolds. *Nat. Method*s 2007, 4, 855-60.[DOI: 10.1038/nmeth1085]

[165] Gao, H.; Korn, J. M.; Ferretti, S.; et al. High-throughput screening using patient-derived tumor xenografts to predict clinical trial drug response. *Nat. Med.* 2015, 21, 1318-25.[DOI: 10.1038/nm.3954]

[166] Tian, Y. F.; Ahn, H.; Schneider, R. S.; et al. Integrin-specific hydrogels as adaptable tumor organoids for malignant B and T cells. *Biomaterials* 2015, 73, 110-9.[DOI: 10.1016/j.biomaterials.2015.09.007]

[167] Duan, Y.; Jin, Y.; Jia, Y.; et al. Fully synthetic nanofibrillar hydrogel for the growth and enzyme-free release of patient-derived ovarian tumor organoids. *Biomaterials* 2026, 326, 123723.[DOI: 10.1016/j.biomaterials.2025.123723]

[168] Gjorevski, N.; Sachs, N.; Manfrin, A.; et al. Designer matrices for intestinal stem cell and organoid culture. *Nature* 2016, 539, 560-4.[DOI: 10.1038/nature20168]

[169] Ng, S.; Tan, W. J.; Pek, M. M. X.; Tan, M.-H.; Kurisawa, M. Mechanically and chemically defined hydrogel matrices for patient-derived colorectal tumor organoid culture. *Biomaterials* 2019, 219, 119400.[DOI: 10.1016/j.biomaterials.2019.119400]

[170] Cruz-Acuña, R.; Kariuki, S. W.; Sugiura, K.; et al. Engineered hydrogel reveals contribution of matrix mechanics to esophageal adenocarcinoma and identifies matrix-activated therapeutic targets. *J. Clin. Invest.* 2023, 133, e168146.[DOI: 10.1172/JCI168146]

[171] Mosquera, M. J.; Kim, S.; Bareja, R.; et al. Extracellular Matrix in Synthetic Hydrogel-Based Prostate Cancer Organoids Regulate Therapeutic Response to EZH2 and DRD2 Inhibitors. *Adv. Mater.* 2022, 34, e2100096.[DOI: 10.1002/adma.202100096]

[172] Rice, A. J.; Cortes, E.; Lachowski, D.; et al. Matrix stiffness induces epithelial-mesenchymal transition and promotes chemoresistance in pancreatic cancer cells. *Oncogenesis* 2017, 6, e352.[DOI: 10.1038/oncsis.2017.54]

[173] Tao, T.; Liu, H.; Gan, Z.; et al. A synthetic hydrogel with tunable stiffness for engineering pancreatic cancer organoids and drug testing. *ACS Biomater. Sci. Eng.* 2025, 11, 5000-11.[DOI: 10.1021/acsbiomaterials.5c00705]

[174] Cavo, M.; Caria, M.; Pulsoni, I.; Beltrame, F.; Fato, M.; Scaglione, S. A new cell-laden 3D Alginate-Matrigel hydrogel resembles human breast cancer cell malignant morphology, spread and invasion capability observed in vivo. *Sci. Rep.* 2018, 8, 5333.[DOI: 10.1038/s41598-018-23250-4]

[175] Jung, Y. H.; Choi, D.-H.; Park, K.; et al. Drug screening by uniform patient-derived colorectal cancer hydro-organoids. *Biomaterials* 2021, 276, 121004.[DOI: 10.1016/j.biomaterials.2021.121004]

[176] Prince, E.; Cruickshank, J.; Ba-Alawi, W.; et al. Biomimetic hydrogel supports initiation and growth of patient-derived breast tumor organoids. *Nat. Commun.* 2022, 13, 1466.[DOI: 10.1038/s41467-022-28788-6]

[177] LeSavage, B. L.; Zhang, D.; Huerta-López, C.; et al. Engineered matrices reveal stiffness-mediated chemoresistance in patient-derived pancreatic cancer organoids. Nat. Mater. 2024, 23, 1138-49.[DOI: 10.1038/s41563-024-01908-x]

[178] Luo, X.; Fong, E. L. S.; Zhu, C.; et al. Hydrogel-based colorectal cancer organoid co-culture models. *Acta Biomater.* 2021, 132, 461-72.[DOI: 10.1016/j.actbio.2020.12.037]

[179] Zhao, Y.; Gong, J.; Liu, H.; Huang, H.; Tan, W. S.; Cai, H. A chemically defined, mechanically tunable, and bioactive hyaluronic acid/alginate double-network hydrogel for liver cancer organoid construction. *Int. J. Biol. Macromol.* 2024, 282, 136707.[DOI: 10.1016/j.ijbiomac.2024.136707]

[180] Jung, M. S.; Poltavets, V.; Skhinas, J. N.; et al. High-throughput 3D engineered paediatric tumour models for precision medicine. *Mol. Syst. Biol.* 2025, 21, 1748-77.[DOI: 10.1038/s44320-025-00152-y]

[181] Miebach, L.; Hagge, M.; Hübner, L.; Bekeschus, S. Protocol for generating a 3D hydrogel-based tumor resection model in vitro using pancreatic cancer cells. *STAR Protoc.* 2026, 7, 104416.[DOI: 10.1016/j.xpro.2026.104416]

[182] Weber, W. A.; Barthel, H.; Bengel, F.; Eiber, M.; Herrmann, K.; Schäfers, M. What Is Theranostics? *J. Nucl. Med.* 2023, 64, 669-70.[DOI: 10.2967/jnumed.123.265670]

[183] Burkett, B. J.; Bartlett, D. J.; McGarrah, P. W.; et al. A Review of Theranostics: Perspectives on Emerging Approaches and Clinical Advancements. *Radiol. Imaging Cancer* 2023, 5, e220157.[DOI: 10.1148/rycan.220157]

[184] van Dam, G. M.; Themelis, G.; Crane, L. M. A.; et al. Intraoperative tumor-specific fluorescence imaging in ovarian cancer by folate receptor-alpha targeting: first-in-human results. *Nat. Med.* 2011, 17, 1315-9.[DOI: 10.1038/nm.2472]

[185] Stummer, W.; Pichlmeier, U.; Meinel, T.; et al. Fluorescence-guided surgery with 5-aminolevulinic acid for resection of malignant glioma: a randomized controlled multicentre phase III trial. *Lancet Oncol.* 2006, 7, 392-401.[DOI: 10.1016/S1470-2045(06)70665-9]

[186] Nguyen, Q. T.; Olson, E. S.; Aguilera, T. A.; et al. Surgery with molecular fluorescence imaging using activatable cell-penetrating peptides decreases residual cancer and improves survival. *Proc. Natl. Acad. Sci. U. S. A.* 2010, 107, 4317-22.[DOI: 10.1073/pnas.0910261107]

[187] Hwang, J.; An, E. K.; Zhang, W.; Kim, H. J.; Eom, Y.; Jin, J. O. Dual-functional alginate and collagen-based injectable hydrogel for the treatment of cancer and its metastasis. J. *Nanobiotechnology* 2022, 20, 245.[DOI: 10.1186/s12951-022-01458-x]

[188] Hwang, J.; Jin, J. O. Attachable Hydrogel Containing Indocyanine Green for Selective Photothermal Therapy against Melanoma. *Biomolecules* 2020, 10, 1124.[DOI: 10.3390/biom10081124]

[189] Rainu, S. K.; Ramachandran, R. G.; Parameswaran, S.; Krishnakumar, S.; Singh, N. Advancements in Intraoperative Near-Infrared Fluorescence Imaging for Accurate Tumor Resection: A Promising Technique for Improved Surgical Outcomes and Patient Survival. *ACS Biomater. Sci. Eng.* 2023, 9, 5504-26.[DOI: 10.1021/acsbiomaterials.3c00828]

[190] Sharma, A.; Verwilst, P.; Li, M.; et al. Theranostic Fluorescent Probes. *Chem. Rev.* 2024, 124, 2699-804.[DOI: 10.1021/acs.chemrev.3c00778]

[191] Luo, H.; Gao, S. Recent advances in fluorescence imaging-guided photothermal therapy and photodynamic therapy for cancer: From near-infrared-I to near-infrared-II. J. Control. *Release* 2023, 362, 425-45.[DOI: 10.1016/j.jconrel.2023.08.056]

[192] Mantooth, S. M.; Green, J. M.; Green, W. D.; et al. An injectable hydrogel enhances intratumoral retention and antitumor efficacy of cytokine immunotherapy in murine triple negative breast tumor models. *J. Control. Release* 2025, 383, 113761.[DOI: 10.1016/j.jconrel.2025.113761]

[193] Vu, T. T.; Jo, S. H.; Kim, S. H.; Kim, B. K.; Park, S. H.; Lim, K. T. Injectable and Multifunctional Hydrogels Based on Poly(N-acryloyl glycinamide) and Alginate Derivatives for Antitumor Drug Delivery. *ACS Appl. Mater. Interfaces* 2024, 16, 15322-35.[DOI: 10.1021/acsami.4c00298]

[194] Liang, S.; Wang, T.; Ding, J.; Yang, J.; He, C.; Rong, Y. Injectable Matrix Metalloproteinase-Responsive Polypeptide Hydrogels as Drug Depots for Antitumor Chemo-Immunotherapy. *Pharmaceutics* 2025, 17, 1453.[DOI: 10.3390/pharmaceutics17111453]

[195] Liu, Z.; Zhang, Y.; Huang, J.; Wang, Y.; Kang, X. In-situ formed thermosensitive hydrogel amplifies statin-mediated immune checkpoint blockade for coordinated tumor chemo-immunotherapy. *Front. Pharmacol.* 2023, 14, 1154392.[DOI: 10.3389/fphar.2023.1154392]

[196] Gierlich, P.; Donohoe, C.; Behan, K.; Kelly, D. J.; Senge, M. O.; Gomes-da-Silva, L. C. Antitumor Immunity Mediated by Photodynamic Therapy Using Injectable Chitosan Hydrogels for Intratumoral and Sustained Drug Delivery. *Biomacromolecules* 2024, 25, 24-42.[DOI: 10.1021/acs.biomac.3c00591]

[197] Wang, Y.; Pan, H.; Meng, Z.; Zhang, C. In Situ Biosynthesis of Photothermal Parasite for Fluorescence Imaging-Guided Photothermal Therapy of Tumors. *Gels* 2022, 8, 754.[DOI: 10.3390/gels8110754]

[198] Xu, Y.; Wang, F.; Liu, W.; et al. Aggregation-Induced-Emission Luminogens Functionalized MXene Nanosheets for Stimuli-Responsive Hydrogel in Pyroptosis-Mediated Choroidal Melanoma Therapy. *Nanomicro Lett.* 2026, 18, 282.[DOI: 10.1007/s40820-026-02077-z]

[199] Heng, C.; Zheng, X.; Hui, J.; Ma, X.; Fan, D. Neodymium and manganese ions co-doped whitlockite for temperature monitoring, photothermal therapy, and bone tissue repair in osteosarcoma. *J. Colloid Interface Sci.* 2024, 653, 1488-503.[DOI: 10.1016/j.jcis.2023.09.186]

[200] Lee, W. T.; Yoon, J.; Kim, S. S.; et al. Combined Antitumor Therapy Using In Situ Injectable Hydrogels Formulated with Albumin Nanoparticles Containing Indocyanine Green, Chlorin e6, and Perfluorocarbon in Hypoxic Tumors. *Pharmaceutics* 2022, 14, 148.[DOI: 10.3390/pharmaceutics14010148]

[201] Qian, Z.; Yuan, Y.; Li, J.; Yuan, W. pH-responsive injectable nanocomposite hydrogel based on dynamic boronate ester bonds loading Pt-TiO_2 nanoparticles and fluorescence probe for synergistic sonodynamic-immunotherapy and imaging of cancer. *J. Mater. Chem. B* 2025, 13, 13635-46.[DOI: 10.1039/d5tb01837d]

[202] Yip, A. M.; Lee, L. C.; Shum, J.; Lo, K. K. A matrix metalloproteinase-responsive iridium(III)-based hydrogel for cancer cell-specific imaging and lysosome-

targeted photodynamic therapy. *Chem. Commun. (Camb.)* 2025, 61, 19461-4.[DOI: 10.1039/d5cc05380c]

[203] Liu, Y.; Li, Y.; Zhang, S.; et al. A PD-L1-targeted and lactate-responsive DNA hydrogel enabling Mito-US therapy: dual functions for postsurgical cancer detection and eradication. *Biomaterials* 2026, 331, 124144.[DOI: 10.1016/j.biomaterials.2026.124144]

[204] Zhang, R.; Ye, Y.; Wu, J.; et al. Immunostimulant In Situ Fibrin Gel for Post-operative Glioblastoma Treatment by Macrophage Reprogramming and Photo-Chemo-Immunotherapy. *ACS Appl. Mater. Interfaces* 2023, 15, 17627-40.[DOI: 10.1021/acsami.3c00468]

[205] Geng, S.; Guo, P.; Wang, J.; et al. Ultrasensitive Optical Detection and Elimination of Residual Microtumors with a Postoperative Implantable Hydrogel Sensor for Preventing Cancer Recurrence. *Adv. Mater.* 2024, 36, e2307923.[DOI: 10.1002/adma.202307923]

[206] Chen, A.; Zhu, J.; Liu, R.; et al. Injectable thermo-sensitive hydrogel enhances anti-tumor potency of engineered Lactococcus lactis by activating dendritic cells and effective memory T cells. *Bioact. Mater.* 2024, 37, 331-47.[DOI: 10.1016/j.bioactmat.2024.03.023]

[207] Wang, Q.; Mei, Y.; Rao, W.; et al. The therapeutic effect of thermo-sensitive hydrogel loaded with recombinant mycobacterium smegmatis expressing exogenous IL-15 in abdominal metastasis. *J. Transl. Med*. 2025, 23, 509.[DOI: 10.1186/s12967-025-06454-x]

[208] Lee, K. K.; Lee, S. C.; Kim, H.; Lee, C. S. Polydopamine nanoparticle-incorporated fluorescent hydrogel for fluorescence imaging-guided photothermal therapy of cancers. *BioChip J.* 2023, 17, 85-92.[DOI: 10.1007/s13206-022-00091-y]

[209] Ranjbar-Navazi, Z.; Fathi, M.; Abdolahinia, E. D.; Davaran, S.; Omidi, Y. MUC-1 aptamer conjugated InP/ZnS quantum dots/nanohydrogel fluorescent composite for mitochondria-mediated apoptosis in MCF-7 cells. *Mater. Sci. Eng. C Mater. Biol. Appl.* 2021, 118, 111469.[DOI: 10.1016/j.msec.2020.111469]

[210] Wang, Y.; Wu, J.; Chen, M.; et al. Application of near-infrared-activated and ATP-responsive trifunctional upconversion nano-jelly for in vivo tumor imaging and synergistic therapy. *Biosens. Bioelectron.* 2024, 250, 116094.[DOI: 10.1016/j.bios.2024.116094]

[211] Bortot, B.; Mangogna, A.; Di Lorenzo, G.; Stabile, G.; Ricci, G.; Biffi, S. Image-guided cancer surgery: a narrative review on imaging modalities and emerging nanotechnology strategies. *J. Nanobiotechnology* 2023, 21, 155.[DOI: 10.1186/s12951-023-01926-y]

[212] Rao, A. D.; Shin, E. J.; Meyer, J.; et al. Evaluation of a Novel Absorbable Radiopaque Hydrogel in Patients Undergoing Image Guided Radiation Therapy for Borderline Resectable and Locally Advanced Pancreatic Adenocarcinoma. *Pract. Radiat. Oncol.* 2020, 10, e508-13.[DOI: 10.1016/j.prro.2020.01.013]

[213] Peng, Z.; Li, M.; Wang, Y.; et al. Self-Assembling Imageable Silk Hydrogels for the Focal Treatment of Osteosarcoma. *Front. Cell Dev. Biol.* 2022, 10, 698282.[DOI: 10.3389/fcell.2022.698282]

[214] Liu, M.; Sun, Y.; Zhou, Y.; et al. A Novel Coacervate Embolic Agent for Tumor Chemoembolization. *Adv. Healthc. Mater.* 2024, 13, e2304488.[DOI: 10.1002/adhm.202304488]

[215] Peng, Y.; Liu, H.; Liang, X.; et al. Self-assembling chemodrug fiber-hydrogel for transarterial chemoembolization and radiotherapy-enhanced antitumor immunity. *J. Control. Release* 2025, 380, 1-16.[DOI: 10.1016/j.jconrel.2025.01.088]

[216] Dong, Y. C.; Nieves, L. M.; Hsu, J. C.; et al. Novel Combination Treatment for Melanoma: FLASH Radiotherapy and Immunotherapy Delivered by a Radiopaque and Radiation Responsive Hydrogel. *Chem. Mater.* 2023, 35, 9542-51.[DOI: 10.1021/acs.chemmater.3c01390]

[217] Delgado, J. F.; Pritchard, W. F.; Varble, N.; et al. X-ray imageable, drug-loaded hydrogel that forms at body temperature for image-guided, needle-based locoregional drug delivery. *Sci. Rep.* 2024, 14, 13352.[DOI: 10.1038/s41598-024-64189-z]

[218] Som, A.; Rosenboom, J. G.; Wehrenberg-Klee, E.; et al. Percutaneous Intratumoral Immunoadjuvant Gel Increases the Abscopal Effect of Cryoablation for Checkpoint Inhibitor Resistant Cancer. *Adv. Healthc. Mater.* 2024, 13, e2301848.[DOI: 10.1002/adhm.202301848]

[219] Huang, G.; Lin, R.; Wang, H.; et al. Magnetosome-incorporated silk fibroin-based magnetic hydrogel for efficient tumor magnetic hyperthermia. *Int. J. Biol. Macromol.* 2025, 334, 148993.[DOI: 10.1016/j.ijbiomac.2025.148993]

[220] Huang, S.; Ma, Z.; Sun, C.; et al. An injectable thermosensitive hydrogel loaded with a theranostic nanoprobe for synergistic chemo-photothermal therapy for multidrug-resistant hepatocellular carcinoma. *J. Mater. Chem. B* 2022, 10, 2828-43.[DOI: 10.1039/d2tb00044j]

[221] Khani, T.; Alamzadeh, Z.; Sarikhani, A.; et al. Fe3O4@Au core-shell hybrid nanocomposite for MRI-guided magnetic targeted photo-chemotherapy. *Lasers Med. Sci.* 2022, 37, 2387-95.[DOI: 10.1007/s10103-021-03486-9]

[222] Huang, Y.; Zhai, X.; Ma, T.; et al. A Unified Therapeutic-Prophylactic Tissue-Engineering Scaffold Demonstrated to Prevent Tumor Recurrence and Overcoming Infection toward Bone Remodeling. *Adv. Mater.* 2023, 35, e2300313.[DOI: 10.1002/adma.202300313]

[223] Park, S. W.; Lai, J. H. C.; Han, X.; et al. Preclinical Application of CEST MRI to Detect Early and Regional Tumor Response to Local Brain Tumor Treatment. *Pharmaceutics* 2024, 16, 101.[DOI: 10.3390/pharmaceutics16010101]

[224] Wu, W. S.; Yan, X.; Chen, S.; et al. Minimally Invasive Delivery of Percutaneous Ablation Agent via Magnetic Colloidal Hydrogel Injection for Treatment of Hepatocellular Carcinoma. *Adv. Mater.* 2024, 36, e2309770.[DOI: 10.1002/adma.202309770]

[225] Shen, Y.; Fan, S.; Wang, B.; et al. Injectable Multifunctional Hydrogel Consisted of Ultrasonic Marker and Immune Adjust Agent in Liver Tumor Ablation: Animal Experiment's Study. *Cardiovasc. Intervent. Radiol.* 2026, 49, 409-21.[DOI: 10.1007/s00270-025-04253-x]

[226] Zhou, Y.; Shu, G.; Luo, Y.; et al. Achieving Complete Tumor Clearance: A Minimalist Manganese Hydrogel for Magnetic Resonance Imaging-Guided Synergetic Microwave Ablation and Chemodynamic Therapy. *Adv. Healthc. Mater.* 2024, 13, e2303268.[DOI: 10.1002/adhm.202303268]

[227] Sampath, B.; Charles, J. Theranostic magnetic hydrogels for treatment, recurrence prevention, tumour modelling and emerging applications in breast cancer management: A review. *Int. J. Biol. Macromol.* 2026, 359, 151874.[DOI: 10.1016/j.ijbiomac.2026.151874]

[228] Ward, K. M.; Aletras, A. H.; Balaban, R. S. A new class of contrast agents for MRI based on proton chemical exchange dependent saturation transfer (CEST). *J. Magn. Reson.* 2000, 143, 79-87.[DOI: 10.1006/jmre.1999.1956]

[229] Li, X.; Ullah, M. W.; Li, B.; Chen, H. Recent Progress in Advanced Hydrogel-Based Embolic Agents: From Rational Design Strategies to Improved Endovascular Embolization. *Adv. Healthc. Mater.* 2023, 12, e2202787.[DOI: 10.1002/adhm.202202787]

[230] Zhang, S.; Lv, R.; Zhang, Z.; Wang, Z.; Jin, Z. Advancements in hydrogel-based embolic agents: Categorized by therapeutic mechanisms. *Cancer Med.* 2024, 13, e70183.[DOI: 10.1002/cam4.70183]

[231] Lee, S. Y.; Choi, J. W.; Hwang, C.; et al. Intravascular casting radiopaque hydrogel systems for transarterial chemo/cascade catalytic/embolization therapy of hepatocellular carcinoma. *Small* 2024, 20, e2400287.[DOI: 10.1002/smll.202400287]

[232] Xu, H.; Ohulchanskyy, T. Y.; Yakovliev, A.; et al. Nanoliposomes Co-Encapsulating CT Imaging Contrast Agent and Photosensitizer for Enhanced, Imaging Guided Photodynamic Therapy of Cancer. *Theranostics* 2019, 9, 1323-35.[DOI: 10.7150/thno.31079]

[233] Lee, S. M.; Yoo, S.-Y.; Kim, T.; et al. Radiopaque hydrogel-in-liposomes towards theranostic applications for malignant tumors. *Biomed. Pharmacother.* 2025, 183, 117822.[DOI: 10.1016/j.biopha.2025.117822]

[234] de Boer, E.; Harlaar, N. J.; Taruttis, A.; et al. Optical innovations in surgery. *Br. J. Surg.* 2015, 102, e56-72.[DOI: 10.1002/bjs.9713]

[235] Kaye, E. A.; Granlund, K. L.; Morris, E. A.; Maybody, M.; Solomon, S. B. Closed-Bore Interventional MRI: Percutaneous Biopsies and Ablations. *AJR Am. J. Roentgenol.* 2015, 205, W400-10.[DOI: 10.2214/AJR.15.14732]

[236] Solomon, S. B.; Silverman, S. G. Imaging in interventional oncology. *Radiology* 2010, 257, 624-40.[DOI: 10.1148/radiol.10081490]

[237] Paefgen, V.; Doleschel, D.; Kiessling, F. Evolution of contrast agents for ultrasound imaging and ultrasound-mediated drug delivery. *Front. Pharmacol.* 2015, 6, 197.[DOI: 10.3389/fphar.2015.00197]

[238] Delgado, J. F.; Owen, J. W.; Pritchard, W. F.; et al. Ultrasound and x-ray imageable poloxamer-based hydrogel for loco-regional therapy delivery in the liver. *Sci. Rep.* 2024, 14, 20455.[DOI: 10.1038/s41598-024-70992-5]

[239] Hou, W.; Mao, W.; Sun, J.; et al. Targeting hydrogel for intelligent recognition and spatiotemporal control in cell-based therapeutics. *Adv. Sci. (Weinh.)* 2024, 11, 2404172.[DOI: 10.1002/advs.202404172]

[240] Zhong, Z.; Chen, Q.; Li, C.; et al. Hydrogel local drug delivery systems for postsurgical management of tumors: Status Quo and perspectives. *Mater. Today Bio* 2024, 29, 101308.[DOI: 10.1016/j.mtbio.2024.101308]

[241] Mohaghegh, N.; Ahari, A.; Zehtabi, F.; et al. Injectable hydrogels for personalized cancer immunotherapies. *Acta Biomater.* 2023, 172, 67-91.[DOI: 10.1016/j.actbio.2023.10.002]

[242] Pacheco, C.; Baião, A.; Ding, T.; Cui, W.; Sarmento, B. Recent advances in long-acting drug delivery systems for anticancer drug. *Adv. Drug Deliv. Rev.* 2023, 194, 114724.[DOI: 10.1016/j.addr.2023.114724]

[243] Alix-Panabières, C.; Pantel, K. Liquid Biopsy: From Discovery to Clinical Application. *Cancer Discov.* 2021, 11, 858-73.[DOI: 10.1158/2159-8290.CD-20-1311]

[244] Liu, L.; Liu, J.; Zhou, W.; et al. An artificial antibody for exosome capture by dull template imprinting technology. *J. Mater. Chem. B* 2022, 10, 6655-63.[DOI: 10.1039/d2tb00494a]

[245] Liu, L.; Dong, C.; Li, X.; et al. Antibody-Free Hydrogel with the Synergistic Effect of Cell Imprinting and Boronate Affinity: Toward the Selective Capture and Release of Undamaged Circulating Tumor Cells. *Small* 2020, 16, e1904199.[DOI: 10.1002/smll.201904199]

[246] Zuo, H.; Jiao, Y.; Chen, J.; Zhao, W. Recent Advances in Smart Stimulus-Responsive Hydrogels for Precision Drug Delivery in Tumours. *Gels* 2026, 12, 98.[DOI: 10.3390/gels12020098]

[247] Ding, H.; Tan, P.; Fu, S.; et al. Preparation and application of pH-responsive drug delivery systems. *J. Control. Release* 2022, 348, 206-38.[DOI: 10.1016/j.jconrel.2022.05.056]

[248] Lee, K. K.; Go, K.; Lee, E.; et al. Multifunctional Hydrogels for Advanced Cancer Treatment: Diagnostic Imaging and Therapeutic Modalities. *Gels* 2025, 11, 426.[DOI: 10.3390/gels11060426]

[249] Xue, W.; Wang, L.; Yi, K.; et al. Hepatocellular carcinoma biomarkers screening based on hydrogel photonic barcodes with tyramine deposition amplified ELISA. *Biosens. Bioelectron*. 2024, 255, 116270.[DOI: 10.1016/j.bios.2024.116270]

[250] Zorrón, M.; Cabrera, A. L.; Sharma, R.; et al. Emerging 2D Nanomaterials-Integrated Hydrogels: Advancements in Designing Theragenerative Materials for Bone Regeneration and Disease Therapy. *Adv. Sci. (Weinh.)* 2024, 11, e2403204.[DOI: 10.1002/advs.202403204]

[251] Rana, M. M.; De la Hoz Siegler, H. Evolution of Hybrid Hydrogels: Next-Generation Biomaterials for Drug Delivery and Tissue Engineering. *Gels* 2024, 10, 216.[DOI: 10.3390/gels10040216]

[252] Cao, L.-Q.; Xie, Y.; Liu, Y.; Wurpel, J.; Zeng, L.; Chen, Z.-S. Application of cancer organoids: The forefront of personalized oncology and preclinical testing. *Organoid Research* 2025, 1, 025050008.[DOI: 10.36922/OR025050008]

[253] Wensink, G. E.; Elias, S. G.; Mullenders, J.; et al. Patient-derived organoids as a predictive biomarker for treatment response in cancer patients. *NPJ Precis. Oncol.* 2021, 5, 30.[DOI: 10.1038/s41698-021-00168-1]